Journal of Medicinal Chemistry

Discovery of *N*-(4-Amino-cyclohexyl)-9-cyclopentyl-*N*-(4-morpholin-4-ylmethyl-phenyl)-9*H*-purine-2,6-diamine as a Potent FLT3 Kinase Inhibitor for Acute Myeloid Leukemia with FLT3 mutations

Tomas Gucky, Eva #ezní#ková, Tereza Radosova Muchova, Radek Jorda, Zuzana Klejova, Veronika Malinkova, Karel Berka, Vaclav Bazgier, HARESH AJANI, Martin Lepsik, Vladimir Divoky, and Vladimir Krystof

J. Med. Chem., **Just Accepted Manuscript** • DOI: 10.1021/acs.jmedchem.7b01529 • Publication Date (Web): 19 Apr 2018

Just Accepted

ACS Publications

is published by the American Chemical Society. 1155 Sixteenth Street N.W., Washington, DC 20036

Discovery of N^2-(4-Amino-cyclohexyl)-9-cyclopentyl-N^6-(4-morpholin-4-ylmethyl-phenyl)-*9H*-purine-2,6-diamine as a Potent FLT3 Kinase Inhibitor for Acute Myeloid Leukemia with FLT3 mutations

Tomáš Gucký[a#], Eva Řezníčková[b#], Tereza Radošová Muchová[c], Radek Jorda[b], Zuzana Klejová[c], Veronika Malínková[a], Karel Berka[d], Václav Bazgier[d], Haresh Ajani,[d,e] Martin Lepšík[e], Vladimír Divoký[c], Vladimír Kryštof[b*]

[a] Department of Chemical Biology and Genetics, Centre of the Region Haná for Biotechnological and Agricultural Research, Faculty of Science, Palacký University, Šlechtitelů 27, 783 71 Olomouc, Czech Republic

[b] Laboratory of Growth Regulators, Centre of the Region Haná for Biotechnological and Agricultural Research, Palacký University and Institute of Experimental Botany AS CR, Šlechtitelů 27, 783 71 Olomouc, Czech Republic

[c] Department of Biology, Faculty of Medicine and Dentistry, Palacký University, Hněvotínská 3, 775 15 Olomouc, Czech Republic

[d] Department of Physical Chemistry, Regional Centre of Advanced Technologies and Materials, Faculty of Science, Palacky University, 17. listopadu 12, 771 46 Olomouc, Czech Republic

[e] Institute of Organic Chemistry and Biochemistry of the Czech Academy of Sciences, Flemingovo nám. 2, 166 10 Prague 6, Czech Republic

[#] These authors contributed equally.

Abstract

FLT3 tyrosine kinase is a potential drug target in acute myeloid leukemia (AML) because patients with FLT3-ITD mutations respond poorly to standard cytotoxic agents and there is a clear link between the disease and the oncogenic properties of FLT3. We present novel 2,6,9-trisubstituted purine derivatives with potent FLT3 inhibitory activity. The lead compound **7d** displays nanomolar activity in biochemical assays and selectively blocks proliferation of AML cell lines harboring FLT3-ITD mutations, whereas other transformed and normal human cells are several orders of magnitude less sensitive. The MV4-11 cells treated with **7d** suppressed the phosphorylation of FLT3 and its downstream signaling pathways, with subsequent G1 cell cycle arrest and apoptosis. Additionally, a single dose of **7d** in mice with subcutaneous MV4-11 xenografts caused sustained inhibition of FLT3 and STAT5 phosphorylation over 48 hours, in contrast to the shorter effect observed after administration of the reference FLT3 inhibitor quizartinib.

Keywords

acute myeloid leukemia, FLT3, kinase inhibitor, docking, drug design

Introduction

Acute myeloid leukemia (AML) is a cancer for which current therapies are inadequate. Recent advances in molecular cancer biology have enhanced our understanding of AML biology and led to the discovery of many cancer-related genes, including potential targets for treatment.[1] The most common mutations in AML occur in the *FLT3* gene; the mutations are observed in approximately 30 % of AML patients and are tightly linked to poor prognosis.[2] The *FLT3* gene encodes the membrane-bound receptor tyrosine kinase FLT3, which is closely related to KIT, FMS and PDGFR.[3] Upon binding to an extracellular ligand, FLT3 dimerizes, gets autophosphorylated, and activates downstream signaling pathways including RAS/MAPK, JAK/STAT5 and PI3K/AKT. These pathways collectively promote growth, proliferation, survival and differentiation of myeloid cells.

The most common group of *FLT3* mutations (found in 23% of all AML patients) are internal tandem duplications (ITD) of variable length and position that promote ligand-independent dimerization.[4] The length of ITD mutations influences prognosis: patients with longer ITDs have worse outcomes and lower overall survival.[5] Point mutations within the activation loop of FLT3 are also somewhat common, occurring in approximately 7 % of all AML cases. These mutations stabilize the kinase in its active conformation and promote constitutive activation.

FLT3 is regarded as a potential drug target because patients with FLT3-ITD mutations respond poorly to standard cytotoxic agents and there is a clear link between AML and the oncogenic properties of FLT3.[6] Consequently, many groups have attempted to develop specific FLT3 inhibitors for AML therapy and a variety of drugs have entered clinical trials.[6-8] Early trials used general receptor tyrosine kinase inhibitors such as sunitinib, sorafenib or lestaurtinib that exhibit activity against FLT3 but were originally developed for other indications.[7] These compounds were quite potent in preclinical experiments, but generally failed in phase I/II clinical trials with AML patients.

The toxicity problems and limited efficacy of these drugs are probably due to their broad specificity towards receptor tyrosine kinases.[7,8] Therefore, new and more specific FLT3 inhibitors have been developed. These so-called second-generation compounds include quizartinib, crenolanib, pexidartinib (PLX3397), tandutinib (MLN518) and gilteritinib (ASP2215). These compounds

demonstrated significant numbers of complete and partial responses in AML patients[7] and are often also active in quizartinib-resistant AML cells with secondary FLT3 point mutations.[9,10]

Some of the developed compounds are multi-targeted anti-FLT3 drugs effective against both AML and other indications. For example, the doubly-selective JAK2/FLT3 inhibitor pacritinib was successful in phase 2 clinical trials against myelofibrosis and lymphoma.[11] Similarly, the clinically tested compound gilteritinib targets FLT3 and AXL,[10] while TG02 (SB1317) inhibits FLT3, JAK2, and all cyclin-dependent kinases (CDKs).[12] The effectiveness of simultaneously targeting FLT3 and CDKs is further demonstrated by the example of AMG 925 (FLX925), which selectively targets FLT3 and CDK4.[13,14] Despite these promising results, acquired resistance to specific FLT3 inhibitors continues to present a major challenge in drug development.

We have previously prepared nanomolar CDK inhibitors with a 6-benzylaminopurine scaffold,[15] but we found that modified analogs (in which the 6-benzylaminopurine core was replaced with a 6-anilinopurine) exhibited substantially reduced cytotoxic activity in most cancer cell lines other than MV4-11 bearing FLT3-ITD mutation. Cells from this line rapidly stopped proliferating and entered G1 phase arrest upon treatment with nanomolar concentrations, whereas the other tested cell lines did not respond to sub-micromolar concentrations. Here we report the preparation of a new set of compounds in this series and demonstrate that their target in the MV4-11 cell line is FLT3.

Results and discussion

Chemistry

The synthesis started from commercially available 2,6-dichloropurine, which was initially alkylated with isopropanol, cyclopentanol or benzyl alcohol *via* the Mitsunobu reaction to obtain 9-substituted-2,6-dichloro-9*H*-purines **1a**,[16] **1b**[15] and **1c**[17] with good regioselectivity. 2,6-dichloro-9-(2-tetrahydropyranyl)-9H-purine (**1d**) was prepared using the previously described reaction of 2,6-dichloro-9*H*-purine with 3,4-dihydro-2H-pyran.[18]

Most of the used 4-substituted-phenylamines were commercially available, but 6-morpholin-4-ylpyridin-3-amine (**4a**) and 4-(2-oxa-6-azaspiro[3.3]hept-6-yl)aniline (**4b**) were prepared by the reaction of 4-bromonitrobenzene (**2a**) or 2-bromo-5-nitropyridine (**2b**) with the corresponding cyclic

secondary amine to yield nitro derivatives (**3a**, **3b**) that were reduced with hydrogen on palladium at atmospheric pressure (see Scheme 1).

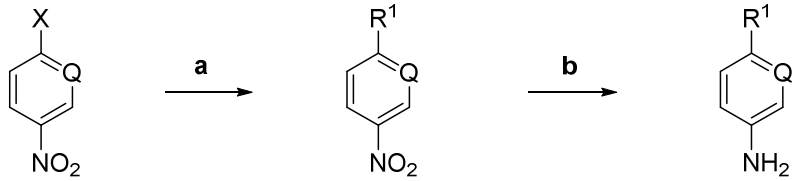

2 **3** **4**

2a: X=Br, Q=CH
2b: X=F, Q=N

3a, 4a: Q=N, R^1=morpholin-4yl
3b, 4b: Q=CH, R^1=2-oxa-6-azaspiro[3.3]hept-6-yl

Scheme 1.

Reaction conditions: a) appropriate secondary amine, K_2CO_3, ethanol, reflux; **b)** H_2/Pd-C 5%, rt, atmospheric pressure.

The nucleophilic substitution at position 6 of the purine moiety with appropriate 4-substituted-aniline or 2-substituted-5-aminopyridine derivatives was performed in the presence of Hünig's base to obtain compounds (**5a-5m**). The substitution of the chlorine at position 2 with a primary or secondary amine was performed with a large excess of the appropriate amine in 1,2-ethandiol at 160 °C. These reactions proceeded smoothly, providing the desired compounds with good yields and high purities (see Scheme 2). We used trans-1,4-diaminocyclohexane for the synthesis of compounds **6a**, **6c**, **6d**, **6h**, **6l**, **7a-7f** and **8l**. The 2-aminopropan-1-ol used for the synthesis of compounds **6b**, **6e**, **6f**, **6i** and **6m** was racemic and for the synthesis of compound **8l** 2-aminobutan-1-ol of R- configuration was used. The collection of newly synthesized compounds (**6a-6o**, **7a-7f,** and **8a-8o)** is presented in Tables 1-3.

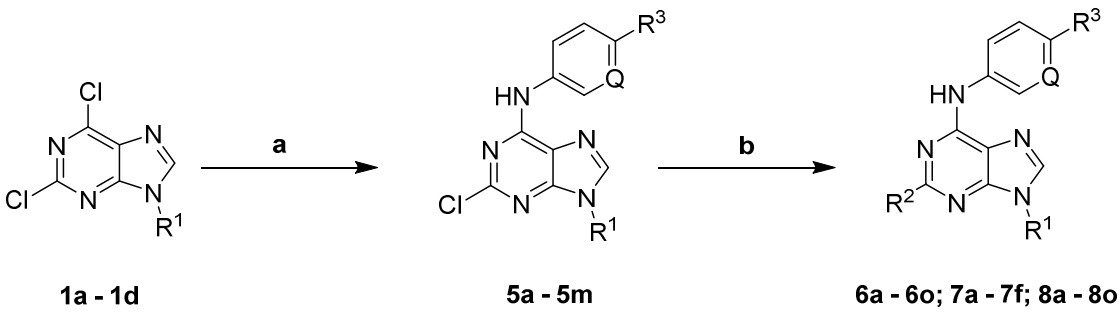

1a - 1d **5a - 5m** **6a - 6o; 7a - 7f; 8a - 8o**

5a: R^1=2-propyl, R^3=Br, Q=CH
5b: R^1=cyclopentyl, R^3=Br, Q=CH
5c: R^1=cyclopentyl, R^3=Cl, Q=CH
5d: R^1=benzyl, R^3=Br, Q=CH
5e: R^1=benzyl, R^3=morpholin-4-yl-methyl, Q=CH
5f: R^1=tetrahydropyran-2-yl, R^3=Br, Q=CH
5g: R^1=cyclopentyl, R^3=pyrrolidin-1-yl, Q=CH
5h: R^1=cyclopentyl, R^3=morpholin-4-yl, Q=CH
5i: R^1=cyclopentyl, R^3=4-ethylpiperazin-1-yl, Q=CH
5j: R^1=cyclopentyl, R^3=morpholin-4-yl-methyl, Q=CH
5k: R^1=cyclopentyl, R^3=2-oxa-6-azaspiro[3.3]hept-6-yl, Q=CH
5l: R^1=cyclopentyl, R^3=4-benzylpiperazin-1-yl, Q=CH
5m: R^1=cyclopentyl, R^3=morpholin-4-yl, Q=N

Scheme 2.

Reaction conditions: a) appropriate 4-substituted aniline or 6-substituted-pyridine-3-amine, DIPEA, n-propanol, 120 °C, 4-20 hours, sealed tube; b) appropriate primary or secondary amine, 1,2-ethandiol, 160 °C, 4-20 hours, sealed tube.

In Vitro Structure–Activity Relationships

The newly prepared 6-(4-substituted-anilino)purine (**6a-6o, 7a-7f, 8a-8o**) and 6-(5-substituted-3-aminopyridine)purine (**8l, 8m**) compounds were tested to determine their ability to inhibit the recombinant FLT3-ITD kinase and to evaluate their antiproliferative activity in the myeloid leukemia MV4-11 (acute; FLT3-ITD-positive) and K562 (chronic; FLT3-negative) cell lines. Tables 1-3 summarize the results obtained.

We began our investigation into the compounds' structure-activity relationships using molecules **6c** and **6d**, which exhibited high selectivity towards FLT3-ITD-positive cells and only weak activity in K562 cancer cell line. Both these compounds have aminocyclohexylamino and 4-halogenophenylamine groups at positions 2 and 6, respectively, with a cyclopentyl group at position 9. To study the impact of substituting position 9 of the purine ring, we compared these initial compounds to a series of analogs with the same substituents at positions 2 and 6 but isopropyl, tetrahydropyran-2-

yl, or benzyl groups at position 9. The lowest GI_{50} values in MV4-11 cells were obtained with compounds bearing isopropyl (**6a**) and cyclopentyl (**6c** and **6d**) substituents (7, 10 and 21 nM, respectively); these compounds were also very potent inhibitors of FLT3-ITD. Introducing the tetrahydropyran-2-yl group (**6l**) reduced both the cellular and kinase-inhibitory activities of the compounds, but the lowest activities were observed for compound **6h**, which has a benzyl group in position 9. To verify the positive impact of substituent 9, we also modified position 2 by replacing the aminocyclohexylamino group with various branched alkylamines (**6e-g**) or bulky morpholino (**6j**) or 4-methyl-piperazin-1-yl (**6k**) moieties. All the analogs substituted in this way had weaker antiproliferative and FLT3-inhibitory activities than the 4-aminocyclohexylamine-substituted compounds, and substantially higher IC_{50} and GI_{50} values (Table 1).

We next explored the effect of extended substituents at position 6. All the compounds tested in these experiments had a cyclopentyl group at position 9 and an aminocyclohexylamino group at position 2 (**7a-7f**, Table 2). The halogen in the phenylamine substituent of the lead molecule was replaced with pyrrolidin-1-yl (**7a**), morpholin-4-yl (**7b**), 4-ethyl-piperazin-1-yl (**7c**), morpholin-4-ylmethyl (**7d**), 2-oxa-6-aza-spiro[3.3]hept-6-yl (**7e**) or N-4-benzyl-piperazin-1-yl (**7f**) moieties. These compounds were among the most active in the entire series: their GI_{50} values in FLT3-ITD positive MV4-11 cells were in the single-digit nanomolar range, and approximately 100 times lower than the corresponding values for K562 cells. They also strongly inhibited the enzymatic activity of FLT3-ITD at low nanomolar concentrations. These results indicate that position 6 can host various substitutions without significant loss of *in vitro* activity (Table 2).

Since the most active compounds of the series (**7b-7d**) have a cyclopentyl group in position 9 and extended 6-(4-substituted-phenylamino) groups, we investigated analogs of these compounds with modifications at position 2 to determine whether the aminocyclohexylamine moiety is the optimal substituent with respect to *in vitro* activity. We investigated linear aminoalkylamines (**8a, 8b, 8c, 8n, 8o**), hydroxyalkylamines (**8i, 8j, 8k**), bulky saturated heterocyclic moieties (**8f, 8g, 8h, 8m**) or aromatic substituents (**8d**, **8e**). Compounds with an 4-aminobutylamine group in position 2 (**8a, 8n, 8o**) showed comparable potency against FLT3-ITD to starting molecules **7d, 7b, 7c** and inhibited MV4-11 proliferation at low nanomolar concentrations, with GI_{50} values of about 11 nM. Longer

aminoalkyl side chains yielded weaker antiproliferative and kinase-inhibitory activities: the FLT3-ITD IC_{50} values for the butyl- (**8a**), pentyl- (**8b**), and hexyl- (**8c**) substituted compounds were 1, 5, and 10 nM, respectively, and the corresponding MV4-11 GI_{50} values were 11, 35, and 86 nM, respectively. Compounds with hydroxyalkylamines in position 2 (**8i, 8j, 8k**) exhibited weaker biological activity: the most potent of these derivatives (**8k**) was 6 times less potent than **7d** with respect to FLT3-ITD inhibition, and had a 40-fold higher GI_{50} value in MV4-11 cells. Shortening of the hydroxyalkyl chain of **8k** (hydroxyethylamine **8i** and hydroxypropylamine **8j**) further reduced their *in vitro* activity. Similarly low activities were achieved with compounds bearing bulky morpholine (**8f**) or methylpiperazine (**8g**) substituents in position 2: the least active compounds in the group were those bearing piperidine (**8h**), benzylamine (**8d**), or 4-methoxybenzylamine (**8e**) moieties (Table 3).

Our synthetic approach allowed us to further modify the first aromatic ring in position 6; we replaced the phenylamine with pyridinamine and extended it with morpholine (**8l**, **8m**). This modification did not improve the molecules' biological activity - for example, compound **8l** displayed similar activity to its phenylamine counterpart **7b** (Tables 2 and 3).

To investigate the cellular selectivity of the new compounds, the antiproliferative activities of the most potent derivatives were tested in cancer cell lines with different histological origins (MOLM-13, Kasumi-1, THP-1, U937, MCF-7, HCC-827) and in noncancerous cells (MRC-5, HUVEC, BJ; Table 4). The compounds exhibited nanomolar activity in the MOLM-13 line (which is FLT3-ITD-positive, like MV4-11), but their GI_{50} values in other cancer cell lines were in the micromolar range, confirming their high selectivity towards FLT3-ITD-positive cells. Notably, Kasumi-1 and HCC-827 cells bearing an activating mutation in c-KIT (Asn822Lys) and an activating deletion in EGFR, respectively, displayed submicromolar sensitivity to compounds **7a-7e**, and compounds from series **8** (**8a-8d, 8o, 8n**) seemed to be even more selective for FLT3-ITD-positive cell lines. Importantly, nontransformed human MRC-5 and HUVEC cells, as well as nonproliferating BJ cells, were not affected by these compounds even when treated with concentrations 1000-fold higher than those toxic against the FLT3-ITD positive MV4-11 and MOLM-13 cell lines.

To further confirm the FLT3-inhibitory effects of our compounds, we evaluated the antiproliferative activity of **7d** in murine Ba/F3 pro-B cells stably transfected with FLT3-ITD. While

the Ba/F3 FLT3-ITD cells were highly sensitive to the **7d** treatment and the GI_{50} values reached low nanomolar concentrations (GI_{50} = 0.034 ± 0.015 μM), in parental Ba/F3 cells the GI_{50} values were higher than 1 μM (GI_{50} = 1.136 ± 0.389). The similar results were obtained using quizartinib as a control (GI_{50} = 0.007 ± 0.003 μM in Ba/F3 FLT3-ITD and 1.452 ± 0.166 μM in parental Ba/F3 cells). Experiments were performed at least in triplicates; for representative graphs see Figure S1.

Table 1. 2-substituted-amino-6-(4-halogenophenyl)amino-9-substituted-9*H*-purines **6a-6o** and their biochemical (recombinant FLT3-ITD) and cellular activities.

	Substituents				**IC_{50} (μM)[a]**	**GI_{50} (μM)[a]**	
	R1	**R2**	**R3**	**Q**	**FLT3 ITD**	**MV4-11**	**K562**
6a	Isopropyl	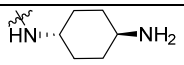	Br	CH	0.010	0.007	1.173
6b	Isopropyl	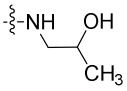	Br	CH	0.591	1.498	17.800
6c	Cyclopentyl	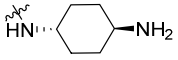	Br	CH	0.004	0.010	0.670
6d	Cyclopentyl	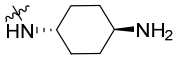	Cl	CH	0.005	0.021	0.840
6e	Cyclopentyl	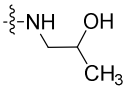	Cl	CH	1.723	0.235	10.910
6f	Cyclopentyl	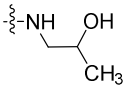	Br	CH	0.628	0.444	>25
6g	Cyclopentyl	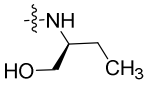	Br	CH	0.281	1.307	7.630
6h	Benzyl	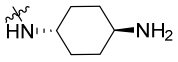	Br	CH	0.798	2.287	3.067
6i	Benzyl	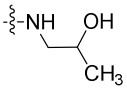	Br	CH	9.848	>4	9.447
6j	Benzyl	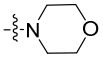	Br	CH	>20	>4	>12.5
6k	Benzyl	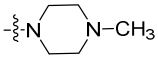	Br	CH	>20	>4	3.800
6l	Tetrahydropyran-2-yl	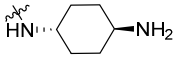	Br	CH	0.070	0.181	5.170

6m	Tetrahydropyran-2-yl	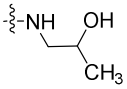	Br	CH	1.141	2.430	27.900
6n	Tetrahydropyran-2-yl	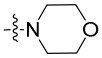	Br	CH	1.195	3.884	3.745
6o	Tetrahydropyran-2-yl	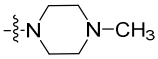	Br	CH	4.207	3.204	7.130

[a] For SD values see Supporting information (Table S1).

Table 2. 2-(4-aminocyclohexylamino)-6-(4-substituted-phenyl)amino-9-cyclopentyl-9*H*-purines **7a-7f** their biochemical (recombinant FLT3-ITD) and cellular activities.

	Substituents				**IC_{50} (μM)[a]**	**GI_{50} (μM)[a]**	
	R1	**R2**	**R3**	**Q**	**FLT3 ITD**	**MV4-11**	**K562**
7a	Cyclopentyl	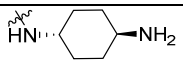		CH	0.003	0.018	0.940
7b	Cyclopentyl	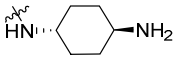	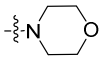	CH	0.002	0.002	0.965
7c	Cyclopentyl	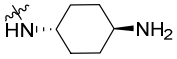	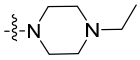	CH	0.003	0.001	2.070
7d	Cyclopentyl	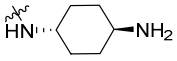	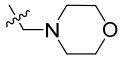	CH	0.003	0.002	0.380
7e	Cyclopentyl	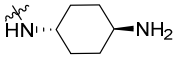		CH	0.004	0.003	1.220
7f	Cyclopentyl	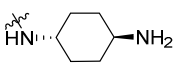	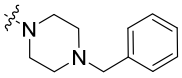	CH	0.006	0.017	0.700

[a] For SD values see Supporting information (Table S1).

Table 3. 9-cyclopentyl-2-substituted-amino-6-arylamino-9*H*-purines **7d, 8a-8o** and their biochemical (recombinant FLT3-ITD) and cellular activities.

	Substituents				**IC_{50} (μM)[a]**	**GI_{50} (μM)[a]**	
	R1	**R2**	**R3**	**Q**	**FLT3 ITD**	**MV4-11**	**K562**
7d	Cyclopentyl	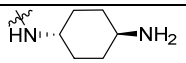	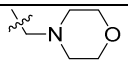	CH	0.003	0.002	0.380
8a	Cyclopentyl	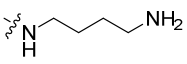	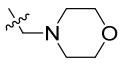	CH	0.001	0.011	2.095

8b	Cyclopentyl	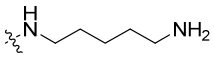	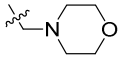	CH	0.005	0.035	1.530
8c	Cyclopentyl	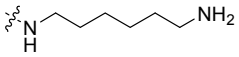	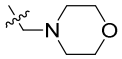	CH	0.010	0.086	3.787
8d	Cyclopentyl	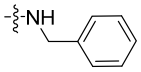	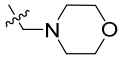	CH	0.026	0.196	3.597
8e	Cyclopentyl	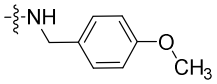	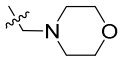	CH	0.209	0.892	6.693
8f	Cyclopentyl	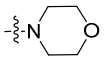	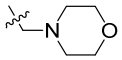	CH	0.019	0.061	4.470
8g	Cyclopentyl	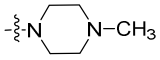	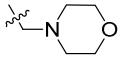	CH	0.053	0.066	2.745
8h	Cyclopentyl		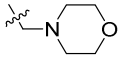	CH	0.050	0.701	11.023
8i	Cyclopentyl	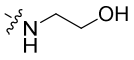	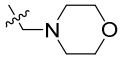	CH	0.029	0.110	2.005
8j	Cyclopentyl	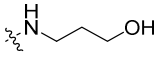	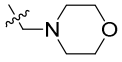	CH	0.047	0.157	2.348
8k	Cyclopentyl	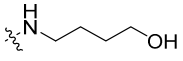	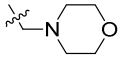	CH	0.018	0.083	1.452
8l	Cyclopentyl	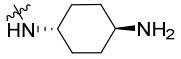	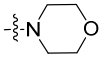	N	0.004	0.004	1.297
8m	Cyclopentyl	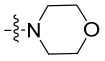	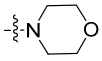	N	0.071	0.070	>25
8n	Cyclopentyl	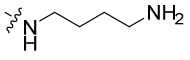	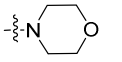	CH	0.004	0.011	3.490
8o	Cyclopentyl	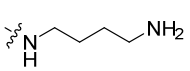	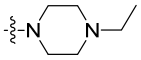	CH	0.001	0.012	1.335
quizartinib					0.010	0.003	>20

[a] For SD values see Supporting information (Table S1).

Table 4. Biochemical (recombinant enzymes) and cellular activities of the most potent compounds.

	IC_{50} (μM)[a]		GI_{50} (μM)[a]								
	FLT3 WT	**FLT3 D835Y**	**MOLM-13**	**Kasumi-1**	**THP-1**	**U937**	**MCF-7**	**HCC-827**	**MRC-5**	**HUVEC**	**BJ**
6c	0.016	0.004	0.015	0.481	2.280	1.797	0.520	1.275	20.628	10.062	14.688
7a	0.021	0.011	0.024	0.569	3.114	3.171	0.487	1.068	14.046	12.077	15.894
7b	0.021	0.007	0.004	0.816	1.159	1.572	0.320	0.521	23.265	4.531	12.249
7c	0.010	0.002	0.004	0.839	0.514	0.605	1.050	0.592	21.964	4.439	12.932
7d	0.013	0.008	0.001	0.513	0.713	0.664	0.197	0.327	20.565	5.866	12.663
7e	0.013	0.028	0.004	0.734	0.693	0.638	1.063	0.456	9.797	5.947	14.580
8a	0.006	0.005	0.019	2.241	3.739	1.341	2.105	1.664	3.878	6.265	10.351
8b	0.025	0.065	0.020	1.283	2.418	3.629	2.120	1.120	5.883	14.165	11.174
8c	0.021	0.069	0.054	1.024	3.590	2.920	5.004	2.248	4.095	10.321	7.265

8d	0.083	0.624	0.122	4.757	>10	9.793	8.600	>5	23.932	10.105	>25
8n	0.023	0.007	0.017	2.016	6.906	4.070	3.255	1.408	7.559	8.058	12.976
8o	0.013	0.003	0.004	2.071	4.355	3.419	2.150	0.976	10.312	11.421	15.389
quiz	0.036	0.136	0.002	0.064	>20	>20	>20	>5	n.t.	n.t.	n.t.

[a] For SD values see Supporting information (Table S2). n.t. – not tested.

Binding mode in FLT3 active site

Kinase inhibitors bind via several types of binding modes, type I and II inhibitors were described for FLT3.[19, 20] Type I inhibitors bind to the ATP binding site, forming hydrogen bonds with the hinge region and presenting substituents in the hydrophobic region near the gatekeeper residue in the active kinase conformation (activation loop-out; DFG-in). In contrast, type II inhibitors bind to the allosteric site in the inactive kinase conformation (DFG-out). Type II FLT3 kinase inhibitors (e.g. quizartinib) were previously structurally characterized in complex with the inactive state of FLT3.[19] The inhibitors in the present study, however, are suggested to have type I binding because of their similar inhibition of WT and D835Y-mutated FLT3 enzymes (Table 4).[21] Due to the unavailability of the structure of the active conformation of FLT3 kinase, we prepared its homology model and docked the lead compound **7d** (see Supporting information**)**. The binding mode is consistent with type I binding, *i.e.* hinge-region hydrogen bonds and 2,6,9-substituents pointing to their respective pockets (Figure 1). In the hinge region, Cys694 backbone forms two classical H-bonds with **7d** (Figure 1) as expected for type I inhibitors. The cyclopentyl ring of **7d** makes hydrophobic contacts with several hydrophobic residues including the Phe691 gatekeeper. The 1,4-diaminocyclohexyl moiety uses its protonated distal 4-amino group to make a salt bridge with Asp829. Further modeling showed that many of the non-hinge-region interactions would be lost in compounds such as **6j**, resulting in a loss of activity. The N atom of the N-methyl morpholino group (pKa of 7.38) loses the proton upon making H-bond with Lys614.

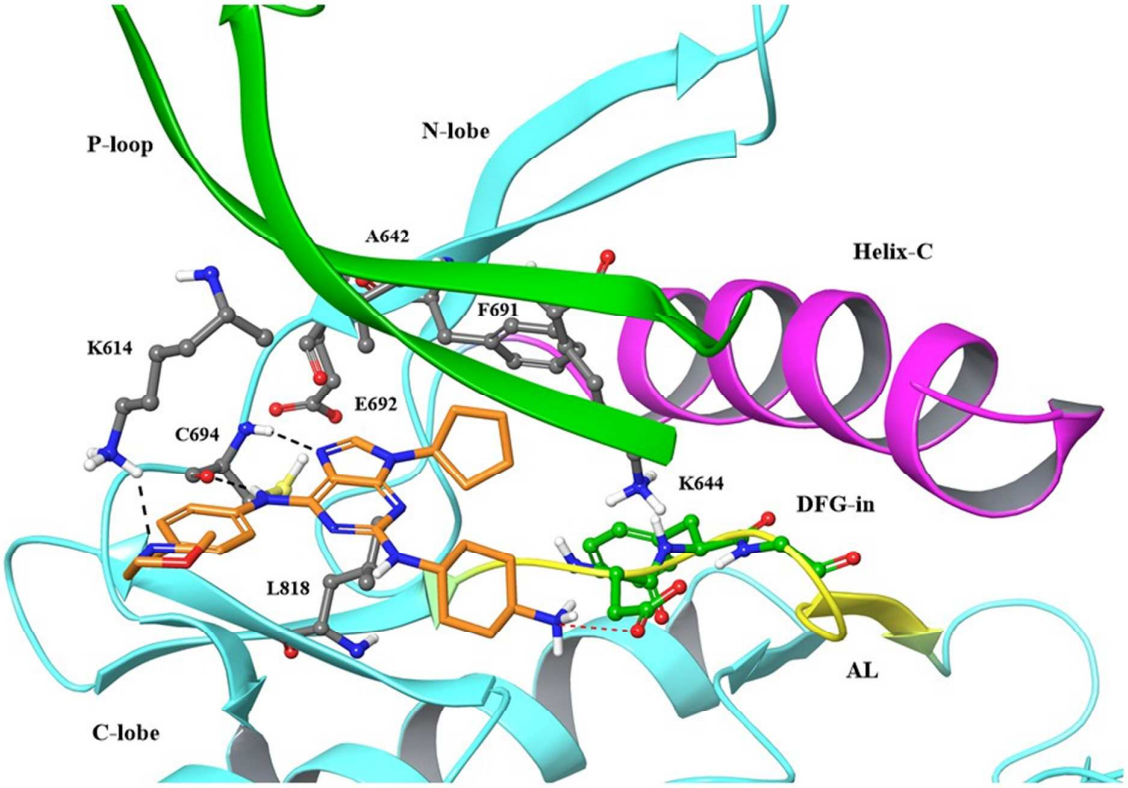

Figure 1. Docked binding pose of **7d** (orange sticks) in FLT3. The kinase (cyan cartoon) is modeled in active conformation; the P-loop (green cartoon), helix-C (magenta) and activation loop (AL; yellow) are highlighted. FLT3 interacting residues are shown as sticks colored grey for carbon, blue for nitrogen, red for oxygen, yellow for sulfur and white for hydrogen. Figure prepared with Maestro, Schrodinger, LLC.

Protein Kinase Selectivity

In addition to FLT3-ITD, most of the active compounds were also potent inhibitors of recombinant wild-type FLT3 and, even more importantly, of a recombinant FLT3 variant bearing the D835Y point mutation, which contributes to the development of resistance (Table 4). Both FLT3-ITD and FLT3-D835Y display similar sensitivity to majority of our compounds, with GI_{50} values in a low nanomolar range. In contrast, quizartinib was at least 10× less potent on D835Y mutant, which is in agreement with published data.[21] Compound **7d**, the most active candidate, was then screened for its activity against 309 protein kinases (Carna Biosciences). This screening confirmed **7d** as a potent inhibitor of

FLT3. It also achieved significant inhibition (>90%) against several other kinases at a concentration of 10 nM, notably PDGFRα/β, CLK1, TRK, QIK, CaMK2δ, SIK, YES, FMS, CAMK2γ, KIT (D816V), MNK2, ACK and SRC (For more details, see the Supporting information Table S3).

Cellular activity of 7d is related to FLT3-inhibition

Because compound **7d** inhibited the proliferation of FLT3-ITD positive MV4-11 and MOLM-13 cell lines very effectively at low nanomolar concentrations (GI_{50} values 2 and 1 nM, respectively), we investigated its molecular mechanism of action in cells. MV4-11 cells were treated for 1 hour with increasing concentrations of the compound and analyzed by immunoblotting, revealing that concentrations as low as 1 nM were sufficient to block the autophosphorylation of the FLT3 receptor tyrosine kinase at three different tyrosine residues (589, 591 and 842). Moreover, this inhibition suppressed phosphorylation of several downstream targets of FLT3. Notably, **7d** abolished phosphorylation of STAT5 at Y694, which is a direct substrate of the oncogenic FLT3-ITD variant. The second pathway affected was the mitogen-activated protein kinase (MAPK) cascade: two key components of this signaling pathway, ERK1/2 (T202/Y204) and MEK1/2 (S217/221), exhibited reduced phosphorylation upon treatment with our compound. **7d** also interfered with PI3K/AKT pathway which was confirmed by reduced phosphorylation of AKT at S473 (Figure 2). Similar results were obtained in MV4-11 cells after treatment with clinically-tested FLT3 inhibitor quizartinib (Figure S3). Because the MAPK and STAT pathways are crucial regulators of cell proliferation, their inhibition induces cell cycle arrest in the G1 phase. To confirm this, MV4-11 cells were treated for 24 hours with increasing doses of compound **7d** and quizartinib, stained with propidium iodide, and analyzed by flow cytometry. Even a 1 nM concentration induced massive G1 arrest. In addition, higher doses increased the number of cells in the sub-G1 phase of the cell cycle, corresponding to an increased number of apoptotic cells (Figure 3A, Figure S4). This result was verified by immunoblotting, which revealed increased cleavage of the apoptotic marker protein PARP-1 (89 kDa fragment) upon treatment with **7d** at 10 or 100 nM for 24 hours. This cleavage was accompanied by reduced levels of the antiapoptotic protein Mcl-1 (Figure 3B). To confirm that the proapoptotic effect

of our compound is closely related to the presence of oncogenic FLT3 variants, we studied the activation of caspases, which play key roles in apoptotic cascades, in MV4-11 (FLT3-ITD) and K562 (no expression of FLT3) cells after treatment with **7d** for 24 hours. Whereas even subnanomolar concentrations of **7d** induced caspase activation in MV4-11, K562 cells were much less sensitive and required vastly greater concentrations for caspase induction (Figure 3C).

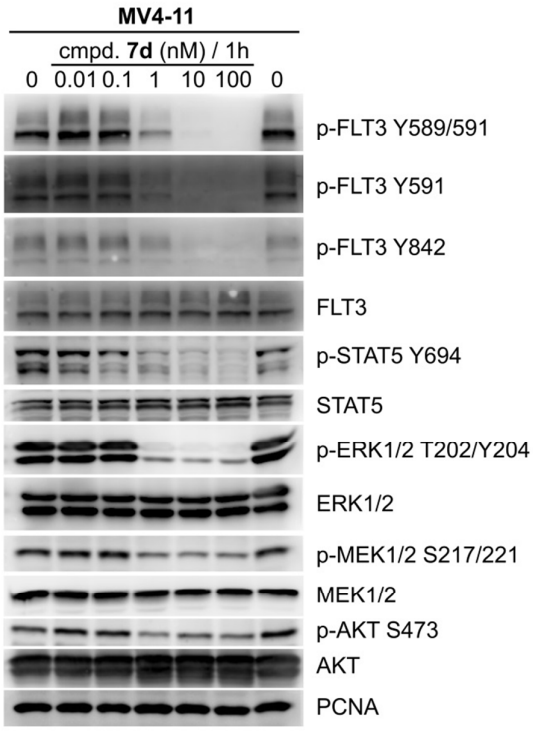

Figure 2. Effect of **7d** on FLT3 and some of its downstream signaling pathways. PCNA was used as a control for protein loading. Densitometric analysis is available from the Supporting information Figure S2.

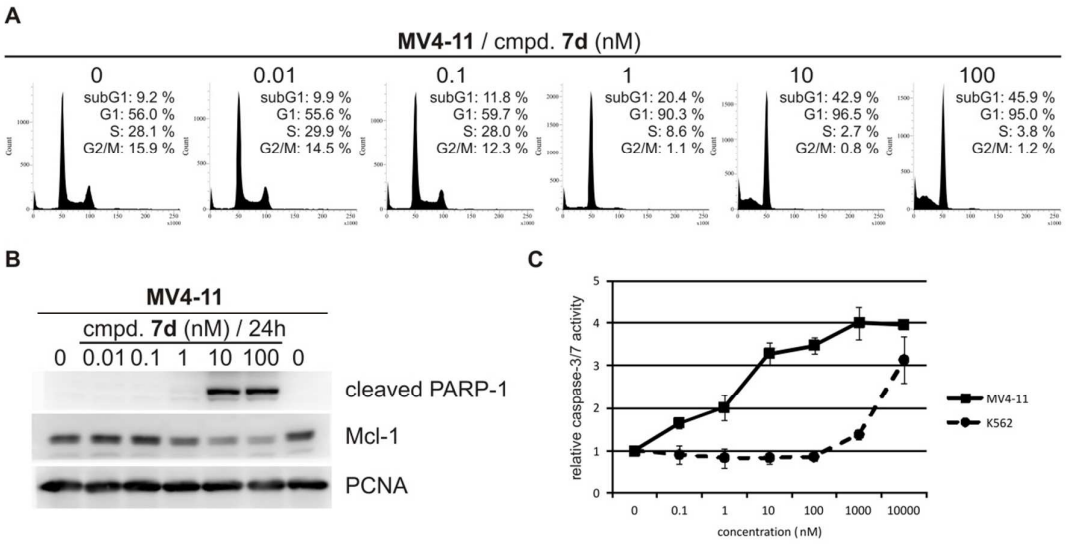

Figure 3. Effect of **7d** on cell cycle (A) and apoptosis (B, C) in the MV4-11 and K562 cell lines.

Activity in MV4-11 xenograft

To determine the efficacy of compound **7d** *in vivo*, we compared its effects to that of quizartinib using human tumor xenografts grown in immunocompromised mice. First, we determined that treatment with **7d** caused no gross toxicity in rats (at doses up to 100 mg/kg i.v. or p.o.; for more details see Supporting information). Next, a single dose of 10 mg/kg of **7d** or quizartinib was administered i.p. to mice with subcutaneously implanted MV4-11 xenografts. Control mice were injected with an equal volume of diluent alone. Tumors were harvested at 4 post-treatment time points: 2, 24, 36, and 48 hours after **7d**, quizartinib, or vehicle injection. The protein lysates were analyzed to detect phosphorylation of the target oncogenic tyrosine kinase FLT3-ITD and its downstream signaling molecules (Figure 4, Figure S5). Compound **7d** effectively inhibited FLT3-ITD autophosphorylation in MV4-11 xenografts (Figure 4A), and unlike quizartinib (Figure 4B),[22-24] it sustained this inhibition of phosphorylation at all analyzed time-points. Next, we investigated the inhibition of the key downstream effectors of FLT3-ITD, namely p-STAT5 and p-ERK1/2 (Figure 4A, B). Treatment with **7d** reduced STAT5 phosphorylation by over 95% after 24 hours, which was a slightly stronger effect than that of quizartinib (Figure S5). Mirroring the results observed for p-FLT3, the suppression of p-

STAT5 phosphorylation induced by **7d** was sustained over 48 hours (Figure 4A), whereas a rebound in STAT5 phosphorylation was detected in lysates from quizartinib-treated tumors (Figure 4B).

In contrast to the results observed for p-STAT5, p-ERK1/2 was only transiently inhibited in the tumor tissue, exhibiting similar rebound kinetics for both tested inhibitors in all animals (Figure 4A, B). Two hours after treatment with **7d** or quizartinib, the suppression of ERK1/2 was reduced by 95% relative to controls (Figure S5). However, its phosphorylation was restored within 24 hours of treatment with either compound, suggesting that there is an adaptive feedback mechanism capable of ERK reactivation in response to FLT3-ITD inhibition. Similar behavior was observed in earlier studies using quizartinib[23] and sorafenib.[25]

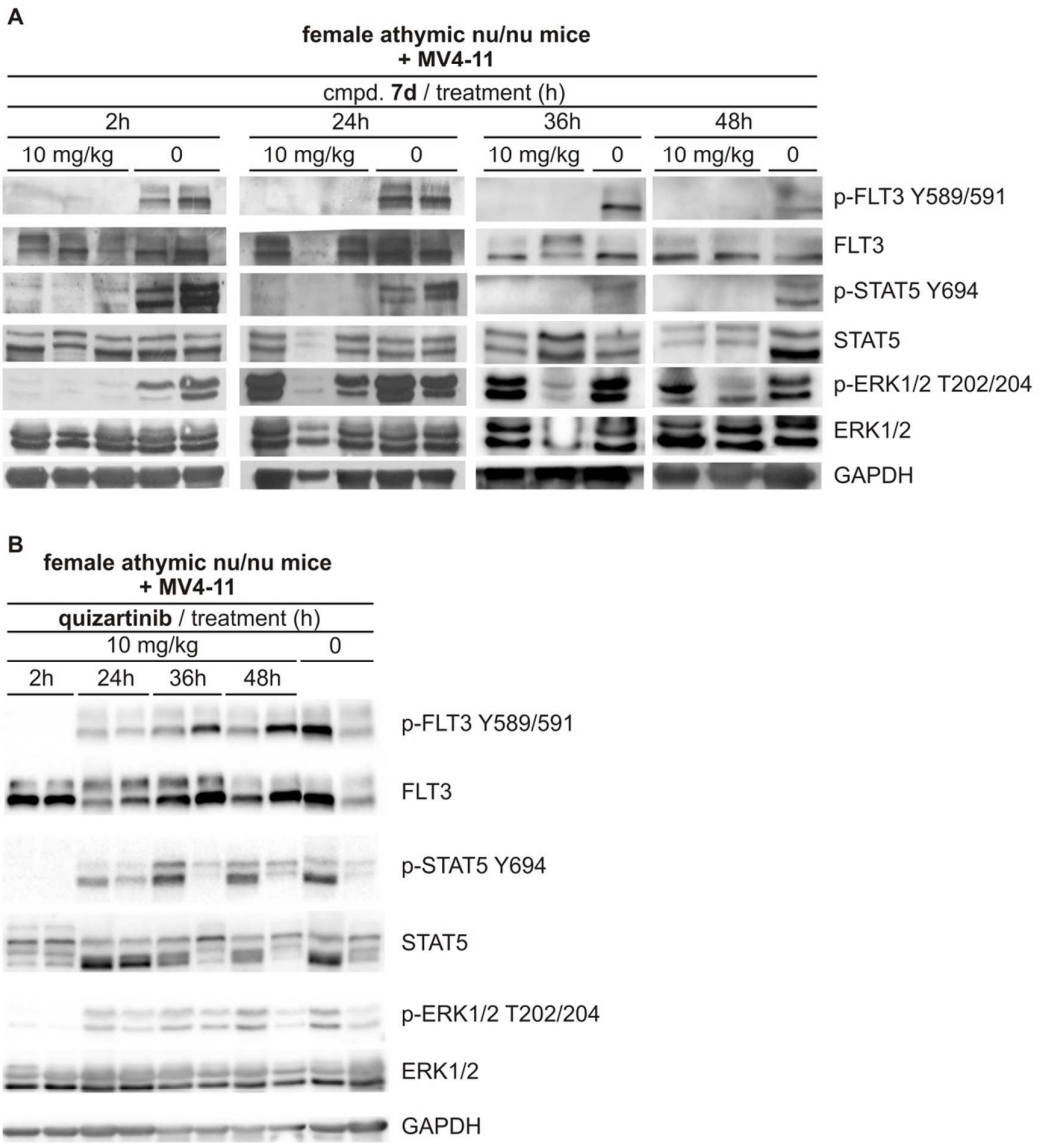

Figure 4. Compound **7d** induces sustained suppression of FLT3-ITD signaling in MV4-11 xenograft tumors. Subcutaneous mouse xenografts were treated with 10 mg/kg **7d** (**A**) or quizartinib (**B**), and the phosphorylation status of FLT3 and its downstream signaling molecules was analyzed by immunoblotting at the indicated times. GAPDH was used as a control for protein loading. Each line represents a separate animal.

Conclusion

We have presented the synthesis of a new generation of highly potent FLT3 inhibitors with a 2,6,9-trisubstutituted purine scaffold. A focused library of 49 compounds was prepared, some members of which exhibited selective nanomolar activity against acute myeloid leukemia cell lines expressing an oncogenic variant of FLT3. The lead compound **7d** inhibited FLT3 autophosphorylation and deactivated its downstream signaling pathways, leading to cell cycle arrest and apoptosis in MV4-11 cells. Docking of **7d** to FLT3 suggests a type I binding mode and explains the structural determinants of its potency. Experiments with subcutaneously implanted MV4-11 xenografts confirmed that a single dose of the tested compound induced sustained inhibition of FLT3 *in vivo*. In conclusion, we suggest this series to be followed for development of potent and specific FLT3 inhibitors for use as drug candidates for treating AML.

Experimental Section

Reagents and General Methods

Chemistry

Melting points were determined on Büchi Melting Point B-540 apparatus and are uncorrected. ^{1}H and ^{13}C-NMR spectra were recorded on a Jeol 500 ECA instrument operating at 500 MHz for ^{1}H and 126 MHz for ^{13}C or on a Bruker Avance 300 spectrometer (300 MHz) at ambient temperature in DMSO-*d6* or $CDCl_3$. Chemical shifts are reported in ppm. Coupling constants (*J*) are reported in Hertz (Hz), and the following abbreviations are used: singlet (s), doublet (d), triplet (t), quartet (q), quintet (qui), sextet (sex), septet (sep), multiplet (m). Mass spectra were recorded using an LCQ ion trap mass spectrometer (Finnigan MAT, San Jose, CA, USA). The chromatographic purity of the compounds was determined using HPLC-DAD-MS. An Alliance 2695 separations module (Waters) linked simultaneously to a PDA 996 (Waters) and a Q-Tof micro (Waters) benchtop quadrupole orthogonal acceleration time-of-flight tandem mass spectrometer were used. Samples were dissolved in methanol and diluted to a concentration of 10 $\mu g \cdot mL^{-1}$ in the mobile phase (initial conditions). Then, 10 µL of the solution were injected on a RP-column (150 mm × 2.1 mm; 3.5 µm; Symmetry C18, Waters). The column was kept in a thermostat at 25 °C. Solvent (A) consisted of 15 mM formic acid adjusted to pH 4.0 with ammonium hydroxide. Methanol was used as the organic modifier (solvent B). At flow rate of 0.2 $mL \cdot min^{-1}$, the following binary gradient was used: 0 min, 10% B; 0–24 min, a linear gradient to 90% B, followed by 10 min isocratic elution of 90% B. At the end of the gradient, the column was re-equilibrated to the initial conditions for 10 min. The effluent was introduced into the DAD (scanning range 210–400 nm, with 1.2 nm resolution) and an electrospray source was applied (source temperature 110 °C, capillary voltage +3.0 kV, cone voltage +20 V, desolvation temperature 250 °C). Nitrogen was used as both the desolvation gas (500 $L \cdot h^{-1}$) and the cone gas (50 $L \cdot h^{-1}$). The mass spectrometer was operated in positive (ESI+) ionization mode, and data were acquired in the 50–1000 m/z range. Elemental analyses were performed using an EA1112 CHN analyser (Thermo Finnigan); the results obtained for C, H, and N were within acceptable limits of the expected values. Merck silica

gel Kieselgel 60 (230–400 mesh) was used for column chromatography. The purity of biologically evaluated compounds was >95% as determined by HPLC-DAD-MS and elemental analysis.

General procedure for the preparation of derivatives 4

4-Fluoronitrobenzene (2a) or 5-bromo-2-nitropyridine (2b) (1.00 mmol), the appropriate secondary amine (1.05 mmol), and potassium carbonate (2.00 mmol) in ethanol (10 mL) were heated under an argon atmosphere in a sealed tube at 100 °C for 4 hours. The completion of the reaction was checked with TLC on silica (chloroform-methanol, 19:1). After cooling to room temperature, the reaction mixture was evaporated under reduced pressure. The residue was partitioned between dichloromethane (25 mL) and water (25 mL). The water phase was extracted twice with dichloromethane (25 mL). The combined organic phases were washed with water, brine, dried over sodium sulphate, and concentrated under reduced pressure. The crude product (3) was then used directly without further purification.

The crude product (3) from the previous step (0.75 mmol) was hydrogenated under atmospheric pressure in methanol (50 mL) with 5% wt. palladium on a charcoal (50 mg). After consumption of hydrogen, the reaction mixture was filtered through celite, washed with methanol and evaporated under reduced pressure. The crude product was dissolved in 2 M hydrochloric acid (50 mL) and extracted with dichloromethane (25 mL). The water phase was neutralised with 5 % sodium hydrogen carbonate, then the precipitate was filtered off and washed with water. The crude product was dried in a vacuum dessicator.

4-(5-Nitro-pyridin-2-yl)-morpholine (3a)

Yield: 85%. Elemental analysis: Calcd.for $C_9H_{11}N_3O_3$ (209.21): C, 51.67; H, 5.30; N, 20.09. Found: C, 51.57; H, 5.48; N, 19.74. HPLC-MS (ESI+): 210.31 (99.8%). GC-MS (EI, M+ (rel.int. m/z)): 209 (18), 124 (100), 87 (28). ^{1}H NMR (500 MHz, $CDCl_3$) δ ppm 2.92-2.98 (m, 4H), 3.71-3.75 (m, 4H), 6.52 (d, J = 9.5, 1H), 8.15 (s, 1H), 9.02 (d, J = 9.5, 1H).

6-(4-Nitro-phenyl)-2-oxa-6-aza-spiro[3.3]heptane (3b)

Yield: 72%. Elemental analysis: Calcd.for $C_{11}H_{12}N_2O_3$ (220.22): C, 59.99; H, 5.49; N, 12.72. Found: C, 59.66; H, 5.12; N, 12.19. HPLC-MS (ESI+): 221.36 (99.7%). GC-MS (EI, M+ (rel.int. m/z)): 220 (21), 150 (100), 120 (57). ^{1}H NMR (500 MHz, DMSO-d_6) δ ppm 4.19-4.21(m, 4H), 4.70-4.72 (m, 4H), 6.44 (d, *J*=9.15, 2H), 8.04 (d, *J* 9.15, 2H).

6-Morpholin-4-yl-pyridin-3-ylamine (4a)

Yield: 98%. Elemental analysis: Calcd.for $C_9H_{13}N_3O$ (179.22): C, 60.32; H, 7.31; N, 23.45. Found: C, 59.96; H, 6.83; N, 23.19. HPLC-MS (ESI+): 180.28 (99.8%). GC-MS (EI, M+ (rel.int. m/z)): 179 (22), 124 (100). ^{1}H NMR (500 MHz, $CDCl_3$) δ ppm 3.05 (s(br, 2H), 3.30-3.34 (m, 4H), 3.79-3.82 (m, 4H), 6.55 (d, *J* = 8.5, 1H), 6.98 (s, 1H), 7.78 (d, *J* = 8.5, 1H).

4-(2-Oxa-6-aza-spiro[3.3]hept-6-yl)-phenylamine (4b)

Yield: 58%. Elemental analysis: Calcd.for $C_{11}H_{14}N_2O$ (190.24): C, 69.45; H, 7.42; N, 14.73. Found: C, 69.13; H, 7.12; N, 14.96. HPLC-MS (ESI+): 191.5 (99.7%). GC-MS (EI, M+ (rel.int. m/z): 190 (11), 132 (100). ^{1}H NMR (500 MHz, DMSO-d_6) δ ppm 3.72-3.75(m, 4H), 4.40 (s (br), 2H), 4.65-4.68 (m, 4H), 6.21 (d, *J*= 8.16, 2H), 6.46 (d, *J*= 8.15, 2H)

General procedure for the preparation of compounds 5a – 5m:

To a suspension of 9-cyclopentyl-2,6-dichloro-9*H*-purine (13) (1.98 mmol) in a mixture of n-propanol (10 mL) and *N,N*-diisopropyl-*N*-ethylamine (8.72 mmol), appropriate amine (2.18 mmol) was added. The suspension was heated with stirring in a sealed tube under an argon atmosphere at 100 °C for 2-6 hours. The reaction was checked by TLC. After completion of the reaction, the reaction mixture was cooled to room temperature and evaporated under reduced pressure. The residue was partitioned between water (50 mL) and dichloromethane (50 mL), and the water phase was extracted two times more with the same volume of dichloromethane. The combined organic phases were washed with water and brine and evaporated under reduced pressure. The crude product was crystallized from petroleum ether:ethyl acetate 3:1.

4-(Bromo-phenyl)-(2-chloro-9-isopropyl-*9H*-purin-6-yl)-amine (5a)

Yield: 89 % m.p.: 154-156 °C. Elemental analysis: Calcd.for $C_{14}H_{13}BrClN_5$ (366.64): C, 45.86; H, 3.57; N, 19.10. Found: C, 45.94; H, 3.81; N, 18.82. HPLC-MS (ESI+): 367.6 (97.8%). ^{1}H NMR (500 MHz, DMSO-d_6) δ ppm 1.49 (d, *J*=7.0, 6H), 4.70 (sep, *J*=7.0, 1H), 7.49 (d, *J*=9.00, 2H), 7.80 (d, *J*=9.00, 2H), 8.44 (s, 1H), 10.39 (s, 1H). ^{13}C NMR (DMSO-d_6, 126 MHz) δ ppm 22.63, 47.49, 115.61, 119.74, 123.45, 131.84, 137.88, 141.17, 150.92, 152.38, 152.69.

4-(Bromo-phenyl)-(2-chloro-9-cyclopentyl-*9H*-purin-6-yl)-amine (5b)

Yield: 85 % m.p.: 193-194 °C. Elemental analysis: Calcd.for $C_{16}H_{15}BrClN_5$ (392.69): C, 48.94; H, 3.85; N, 17.83. Found: C, 49.06; H, 3.94; N, 17.49. HPLC-MS (ESI+): 393.7 (98.4%). ^{1}H NMR (300 MHz, DMSO-d_6) δ ppm 1.87-1.92 (m, 2H), 1.92-1.99 (m, 4H), 2.01-2.23 (m, 2H), 4.85 (qui, *J*=7.17, 1H), 7.54 (d, *J*=8.73, 2H), 7.84 (d, *J*=8.73, 2H), 8.45 (s, 1H), 10.42 (s, 1H).

(2-Chloro-9-cyclopentyl-*9H*-purin-6-yl)-(4-chloro-phenyl)-amine (5c)

Yield: 78 % m.p.: 212-214 °C. Elemental analysis: Calcd.for $C_{16}H_{15}Cl_2N_5$ (348.24): C, 55.19; H, 4.34; N, 20.11. Found: C, 55.56; H, 4.05; N, 19.89. HPLC-MS (ESI+): 349.4 (96.4%). ^{1}H NMR (300 MHz, DMSO-d_6) δ ppm 1.67-1.71(m, 2H), 1.72-1.76(m, 4H), 1.89-2.20 (m, 2H), 4.84 (sep, *J*= 7.17, 1H), 7.40 (d, *J*= 8.85, 2H), 7.89(d, *J*= 8.85, 2H), 8,44 (s, 1H), 10.43 (s, 1H).

(9-Benzyl-2-chloro-*9H*-purin-6-yl)-(4-bromo-phenyl)-amine (5d)

Yield: 54 % m.p.: 231-233 °C. Elemental analysis: Calcd.for $C_{18}H_{13}BrClN_5$ (414.69): C, 52.13; H, 3.16; N, 16.89. Found: C, 52.02; H, 3.45; N, 16.93. HPLC-MS (ESI+): 415.8 (97.8%). ^{1}H NMR (500 MHz, DMSO-d_6) δ ppm 5.53 (s, 2H), 7.31-7.42 (m, 5H), 7.56 (d, *J*=8.43, 2H), 8.03 (d, *J*=8.43, 2H), 8.87 (s, 1H), 9.25 (s(br), 1H).

(9-Benzyl-2-chloro-*9H*-purin-6-yl)-(4-morpholin-4-ylmethyl-phenyl)-amine (5e)

Yield: 76 %. m.p.: 194-196 °C. Elemental analysis: Calcd.for $C_{23}H_{23}ClN_6O$ (434.93): C, 63.52; H, 5.33; N, 19.32. Found: C, 63.82; H, 5.12; N, 19.01. HPLC-MS (ESI+): 435.9 (96.2%). ^{1}H NMR (300 MHz, DMSO-d_6) δ ppm 2.35-2.41 (m, 4H), 3.43 (s, 2H), 3.60 (t, *J*=7.85, 4H), 5.41 (s, 2H), 7.26-7.37 (m, 7H), 7.76 (d, *J*=8.40, 2H), 8.43 (s, 1H), 10.34 (s, 1H). ^{13}C NMR (76 MHz, DMSO-d_6) δ ppm 46.95, 53.64, 62.51, 66.69, 119.26, 121.68, 127.98, 128.43, 129.34, 129.69, 133.32, 137.09, 138.11, 142.85, 151.23, 152.94, 153.08.

(4-Bromo-phenyl)-[2-chloro-9-(tetrahydro-pyran-2-yl)-*9H*-purin-6-yl]-amine (5f)

Yield: 76 %. m.p.: 143-144 °C. Elemental analysis: Calcd.for $C_{16}H_{15}BrClN_5O$ (408.69): C, 47.02; H, 3.70; N, 17.14. Found: C, 47.13; H, 3.44; N, 17.11. HPLC-MS ESI+): 410.2 (97.5%). ^{1}H NMR (300 MHz, DMSO-d_6) δ ppm 1.55-1.58(m, 2H), 1.73-1.76 (m, 1H), 1.95-1.99 (m, 2H), 2.20 (t, *J*=5.3, 1H), 3.67-3.75 (m, 1H), 4.00 (d, *J*=5.3, 1H), 5.63 (d, *J*=10.71, 1H), 7.54 (d, *J*=8.79, 2H), 7.82 (d, *J*=8.79, 2H), 8.58 (s, 1H), 10.49 (s(br), 1H). ^{13}C NMR (76 MHz, DMSO-d_6) δ ppm 22.19, 24.39, 29.81, 67.61, 80.90, 115.19, 118.78, 122.95, 131.25, 138.09, 140.53, 150.22, 152.09, 152.34

(2-Chloro-9-cyclopentyl-*9H*-purin-6-yl)-(4-pyrrolidin-1-yl-phenyl)-amine (5g)

Yield: 92%. m.p.: 168-169 °C. Elemental analysis: Calcd.for $C_{20}H_{23}ClN_6$ (382.89): C, 62.74; H, 6.05; N, 21.95. Found: C, 62.54; H, 5.82; N, 21.83. HPLC-MS (ESI+): 384 (99.9%). ^{1}H NMR (500 MHz, DMSO-d_6) δ ppm 1.63-1.81(m, 2H), 1.86-1.99 (m, 8H), 2.14-2.21 (m, 2H), 3.19-3.23 (m, 4H), 4.81 (qui, *J*=7.17, 1H), 6.49 (d, *J*=8.73, 2H), 7.49 (d, *J*=8.73, 2H), 8.28 (s, 1H), 9.89(s, 1H). ^{13}C NMR (126 MHz, DMSO-d_6) δ ppm 24.03, 25.47, 32.57, 48.02, 55.97, 111.85, 119.27, 123.95, 127.55, 140.56, 145.38, 150.70, 152.90, 153.19.

(2-Chloro-9-cyclopentyl-*9H*-purin-6-yl)-(4-morpholin-4-yl-phenyl)-amine (5h)

Yield: 72%. m.p.: 145-148 °C. Elemental analysis: Calcd.for $C_{20}H_{23}ClN_6O$ (398.89): C, 60.22; H, 5.81; N, 21.07. Found: C, 60.25; H, 5.88; N, 21.19. HPLC-MS (ESI+): 400.7 (98.5%). ^{1}H NMR (300 MHz, $CDCl_3$) δ ppm 1.79-1.83 (m, 2H), 1.85-1.96 (m, 4H), 2.27-2.36 (m, 2H), 3.14-3.18 (m, 4H), 3.88-3.90 (m, 4H), 4.94 (qui, *J*=7.32, 1H), 6.97 (d, *J*=8.94, 2H), 7.65 (d, *J*=8.94, 2H), 7.80 (s (br),

1H), 7.83 (s, 1H). ^{13}C NMR (126 MHz, DMSO-d_6) δ ppm 23.91, 33.04, 49.89, 55.97, 66.96, 116.54, 119.28, 121.89, 130.84, 138.78, 148.11, 150.70, 152.48, 154.03.

2-Chloro-9-cyclopentyl-*9H*-purin-6-yl)-[4-(4-ethyl-piperazin-1-yl)-phenyl]-amine (5i)

Yield: 82%. m.p.: 128-131 °C. Elemental analysis: Calcd.for $C_{22}H_{28}ClN_7$ (425.96): C, 62.03; H, 6.63; N, 23.02. Found: C, 61.93; H, 6.79; N, 23.22. HPLC-MS (ESI+): 427.3 (99.5%). ^{1}H NMR (300 MHz, $CDCl_3$) δ ppm 1.16 (t, *J*=7.2, 3H), 1.65-1.68 (m, 2H), 1.83-1.95 (m, 4H), 2.26-2.32 (m, 2H), 3.05-3.11 (m, 4H), 3.27-3.35 (m, 4H), 4.78 (qui, *J*=6.9, 1H), 6.89 (d, *J*=9.00, 2H), 7.57 (d, *J*=9.00, 2H), 8.32 (s, 1H), 10.02 (s, 1H). ^{13}C NMR (300 MHz, $CDCl_3$) δ ppm 11.27, 24.24, 24.45, 32.19, 32.32, 54.84, 55.48, 63.33, 113.59, 114.68, 122.36, 131.50, 137.37, 140.41, 152.24, 159.16.

(2-Chloro-9-cyclopentyl-*9H*-purin-6-yl)-(4-morpholin-4-ylmethyl-phenyl)-amine (5j)

Yield: 69%. m.p.: 123-124 °C. Elemental analysis: Calcd.for $C_{21}H_{25}ClN_6O$ (412.92): C, 61.08; H, 6.10; N, 20.35. Found: C, 61.33; H, 5.99; N, 20.02. HPLC-MS (ESI+): 414.2 (99.5%). ^{1}H NMR (300 MHz, $CDCl_3$) δ ppm 1.78-1.82 (m, 2H), 1.84-1.99 (m, 4H), 2.28-2.36 (m, 2H), 2.47-2.52 (m, 4H), 3.53 (s, 2H), 3.70-3.74 (m, 4H), 4.95 (qui, *J*=5.4, 1H), 7.37(d, *J*=8.22, 2H), 7.74 (d, *J*=8.22, 2H), 7.86 (s, 1H). ^{13}C NMR (300 MHz, $CDCl_3$) δ ppm 23.93, 33.04, 53.51, 56.04, 62.92, 67.06, 119.52, 120.01, 129.42, 132.12, 137.29, 139.07, 150.87, 152.30, 153.87.

2-Chloro-9-cyclopentyl-*9H*-purin-6-yl)-[4-(2-oxa-6-aza-spiro[3.3]hept-6-yl)-phenyl]-amine (5k)

Yield: 74%. m.p.: 119-120 °C. Elemental analysis: Calcd.for $C_{21}H_{23}ClN_6O$ (410.90): C, 61.38; H, 5.64; N, 20.45. Found: C, 61.14; H, 5.39; N, 20.19. HPLC-MS (ESI+): 411.9 (97.7%). ^{1}H NMR (300 MHz, DMSO-d_6) δ ppm 1.67-1.72 (m, 2H), 1.84-1.99 (m, 4H), 2.11-2.18 (m, 2H), 3.92-3.94 (m, 4H), 4.70-4.72(m, 4H), 4.81 (qui, *J*= 5.4, 1H), 6.43 (d, *J*=8.70, 2H), 7.53 (d, *J*=8.70, 2H), 8.33 (s, 1H), 9.99 (s, 1H).

[4-(4-Benzyl-piperazin-1-yl)-phenyl]-(2-chloro-9-cyclopentyl-9*H*-purin-6-yl)-amine (5l)

Yield: 79 %. m.p. 181-182 °C. Elemental analysis: Calcd.for $C_{27}H_{30}ClN_7$ (488.03): C, 66.45; H, 6.20; N, 20.09. Found: C, 66.71; H, 6.41; N, 19.84. HPLC-MS (ESI+): 490.6 (99.9%). ^{1}H NMR (DMSO-d_6, 500 MHz) δ ppm 1.62-1.70 (m, 2H), 1.79-1.86 (m, 2H), 1.89-1.97 (m, 2H), 2.10-2.16 (m, 2H), 3.06-3.09 (m, 4H), 3.29-3.31 (m, 4H), 3.49 (s, 2H), 4.78 (qui, *J*=7.5, 1H), 6.88 (d, *J*=9.0, 2H), 7.21-7.25 (m, 1H), 7.27-7.31 (m, 4H), 7.57 (d, *J*=9.0, 2H), 8.32 (s, 1H), 10.03 (s, 1H). ^{13}C NMR (126 MHz, DMSO-d_6) δ ppm 24.03, 32.56, 49.14, 53.09, 56.01, 62.60, 115.99, 119.38, 123.13, 127.51, 128.74, 129.46, 130.91, 138.61, 140.84, 148.10, 150.85, 152.76, 152.99.

2-Chloro-9-cyclopentyl-*9H*-purin-6-yl)-(6-morpholin-4-yl-pyridin-3-yl)-amine (5m)

Yield: 88%. m.p. 113-115 °C. Elemental analysis: Calcd.for $C_{19}H_{22}ClN_7O$ (399.88): C, 57.07; H, 5.55; N, 24.52. Found: C, 57.23; H, 5.21; N, 24.14. HPLC-MS (ESI+): 400.9 (99.5%). ^{1}H NMR (500 MHz, DMSO-d_6) δ ppm 1.79-1.83 (m, 2H), 1.85-1.96 (m, 4H), 2.27-2.36 (m, 2H), 3.14-3.18 (m, 2H), 3.88-3.90 (m, 2H), 4.91 (qui, *J*=6.55, 1H), 6.93 (s, 1H), 7.41-7.47 (m, 2H), 7.98 (s, 1H), 8.25 (s(br), 1H).

General procedure for the preparation of compounds 6a-6o, 7a-7f and 8a-8o:

The mixture of 2-chloro-9-cyclopentyl-9*H*-purin-6-subst.amino derivative 15 (1.00 mmol) and trans-1,4-diaminocyclohexane (10.0 mmol) in 1,2-ethandiole (5,0 mL) was heated with stirring at 160 °C for 4 hours in an argon atmosphere. After cooling to room temperature, the mixture was diluted with ethyl acetate (40 mL) and washed with water (40 mL). The organic phase was washed with brine, dried over sodium sulphate and concentrated under reduced pressure. The crude product was purified by column chromatography on silica using mobile phase chloroform – methanol (4:1, v/v).

***N*^{2}-(4-Amino-cyclohexyl)-*N*^{6}-(4-bromo-phenyl)-9-isopropyl-9H-purine-2,6-diamine (6a)**

Yield: 85 %. m.p.: 224-226 °C. Elemental analysis: Calcd. for $C_{20}H_{26}BrN_7$ (444.37): C, 54.06; H, 5.90; N, 22.06. Found: C, 53.99; H, 5.73; N, 22.23. HPLC-MS (ESI+): 446.0 (97.9%). ^{1}H NMR (500 MHz, DMSO-d_6) δ ppm 1.07 – 1.29 (m, 4H), 1.45 (d, *J* = 6.4, 6H), 1.77 (d, *J* = 11.8, 2H), 1.93 (d, *J* = 11.5, 2H), 3.64 – 3.52 (m, 2H), 4.59 – 4.49 (sep, *J*=6.50, 1H), 6.47 (s(br), 1H), 7.39 (d, *J* = 8.7, 2H), 7.91 (s,

1H), 7.99(d, *J*=8.7, 2H), 9.55 (s(br), 1H). ^{13}C NMR (126 MHz, DMSO-d_6) δ ppm 22.57, 31.84, 35.76, 46.29, 50.56, 113.53, 114.40, 122.17, 131.42, 136.69, 140.54, 152.20, 158.59.

1-[6-(4-Bromo-phenylamino)-9-isopropyl-9H-purin-2-ylamino]-propan-2-ol (6b)

Yield: 79 %. m.p.: 178-180 °C. Elemental analysis: Calcd. For $C_{17}H_{21}BrN_6O$ (405.30): C, 50.38; H, 5.22; N, 20.74. Found: C, 50.59; H, 5.49; N, 20.58. HPLC-MS (ESI+): 407.0 (98.1%). ^{1}H NMR (500 MHz, DMSO-d_6) δ ppm 1.06 (d, *J* = 6.2, 3H), 1.46 (d, *J* = 6.8, 6H), 3.20 – 3.12 (m, 1H), 3.30 – 3.23 (m, 2H), 3.81(sep, *J* = 5.5, 1H), 4.55 (sep, *J* = 7.0, 1H), 4.70 (s, 1H), 6.50 (t, *J* = 5.8, 1H), 7.39 (d, *J* = 8.9, 2H), 7.93 (s, 1H), 7.97 (d, *J* = 8.7, 2H), 9.55 (s(br), 1H). ^{13}C NMR (126 MHz, DMSO-d_6) δ ppm 21.93, 22.56, 46.40, 49.82, 65.92, 113.66, 114.68, 122.40, 131.49, 136.78, 140.38, 151.87, 152.24, 159.30.

***N*^{2}-(4-Amino-cyclohexyl)-*N*^{6}-(4-bromo-phenyl)-9-cyclopentyl-9*H*-purine-2,6-diamine (6c)**

Yield: 79 %. m.p.: 162-164 °C. Elemental analysis: Calcd. For $C_{22}H_{28}BrN_7$ (470.42): C, 56.17; H, 6.00; N, 20.84. Found: C, 56.39; H, 5.63; N, 20.51. HPLC-MS (ESI+): 473.0 (99.8%). ^{1}H NMR (300 MHz, DMSO-d_6) δ ppm 1.09-1.32 (m, 4H), 1.64-1.68 (m, 2H), 1.78-2.08 (m, 12H), 2.57 (m, 1H), 3.58-3.61 (m, 1H), 4.69 (qui, *J*=7.11, 1H), 6.50 (d, *J*=7.41, 1H), 7.42 (d, *J*=8.85, 2H), 7.90 (s, 1H), 8.04 (d, *J*=8.85, 2H), 9.58 (s (br), 1H). ^{13}C NMR (76 MHz, DMSO-d_6) δ ppm 24.18, 24.48, 31.77, 32.28, 35.67, 49.12, 50.63, 133.53, 122.22, 123.80, 131.42, 137.46, 140.55, 150.85, 152.26, 158.52.

***N*^{2}-(4-Amino-cyclohexyl)-*N*^{6}-(4-chloro-phenyl)-9-cyclopentyl-*9H*-purine-2,6-diamine (6d)**

Yield: 84 % m.p.: 113-115 °C. Elemental analysis: Calcd. for $C_{22}H_{28}ClN_7$ (425.96): C, 62.03; H, 6.63; N, 23.02. Found: C, 61.87; H, 6.89 N, 21.31. HPLC-MS (ESI+): 426.2 (98.7%). ^{1}H NMR (500 MHz, DMSO-d_6) δ ppm 1.29–1.04 (m, 4H), 1.68–1.56 (m, 2H), 2.11 – 1.72(m, 10H), 2.56–2.48 (m, 1H), 3.62 – 3.52 (m, 1H), 4.65 (qui, *J* = 6.3, 1H), 6.48 (d, *J* = 4.9, 1H), 7.26 (d, *J* = 8.5, 2H), 7.87 (s, 1H), 8.06 (d, *J* = 8.8, 2H), 9.54 (s(br), 1H). ^{13}C NMR (126 MHz, DMSO-d_6) δ ppm 24.29, 31.77, 32.28, 35.67, 50.56, 50.78, 55.50, 114.48, 121.80, 125.55, 128.51, 137.40, 140.13, 152.27, 158.52.

1-[6-(4-Chloro-phenylamino)-9-cyclopentyl-*9H*-purin-2-ylamino]-propan-2-ol (6e)

Yield: 79 % m.p.: 128-129 °C. Elemental analysis: Calcd. for $C_{19H23}ClN_6O$ (386.88): C, 58.99; H, 5.99; N, 21.72. Found: C, 58.63; H, 6.22 N, 21.94. HPLC-MS (ESI+): 387.3 (98.7%). ^{1}H NMR (300 MHz, DMSO-d_6) δ ppm 1.09 (d, *J*= 6.18, 3H), 1.63-1.67 (m, 2H), 1.87-2.00 (m, 4H), 2.09-2.21 (m, 2H), 3.14-3.22 (m, 2H), 3.75-3.89 (m, 1H), 4.67 (sep, *J*= 7.41, 1H), 4.72 (s(br), 1H), 6.54 (t, *J*= 5.19, 1H), 7.30 (d, *J*= 8.67, 2H), 7.89 (s, 1H), 8.06 (d, *J*=8.67, 2H), 9.58 (s, 1H). ^{13}C NMR (DMSO-d_6, 76 MHz) δ ppm 21.29, 23.63, 31.66, 49.20, 54.81, 65.28, 114.12, 121.36, 125.07, 127.96, 136.74, 139.33, 151.67, 158.67.

1-[6-(4-Bromo-phenylamino)-9-cyclopentyl-*9H*-purin-2-ylamino]-propan-2-ol (6f)

Yield: 94 %. m.p.: 133-134 °C. Elemental analysis: Calcd. for $C_{19}H_{23}BrN_6O$ (431.33): C, 52.91; H, 5.37; N, 19.48. Found: C, 52.84; H, 5.19 N, 19.56. HPLC-MS (ESI+): 433.0 (98.0%). ^{1}H NMR (500 MHz, DMSO-d_6) δ ppm 1.05 (d, *J*= 6.23, 3H), 1.62-1.67 (m, 2H), 1.80-1.86 (m, 2H), 1.92-1.97 (m, 2H), 2.04-2.09 (m, 2H), 3.11-3.17 (m, 1H), 3.25-3.29 (m, 1H), 3.81 (sep, *J*=5.8, 1H), 4.63-4.68 (m, 2H), 6.51 (t, *J*= 5.28, 1H), 7.39 (d, *J*= 8.85, 2H), 7.89 (s, 1H), 7.99 (d, *J*=8.85, 2H), 9.56 (s, 1H). ^{13}C NMR (DMSO-d_6, 126 MHz) δ ppm 21.95, 24.27, 32.31, 49.83, 55.42, 60.25, 65.88, 113.64, 114.78, 122.43, 131.48, 137.40, 140.41, 152.28, 159.27.

(*R*)-3-[6-(4-Bromo-phenylamino)-9-cyclopentyl-*9H*-purin-2-ylamino]-2-methyl-propan-1-ol (6g)

Yield: 85 %. m.p.: 156-158 °C. Elemental analysis: Calcd. for $C_{20}H_{25}BrN_6O$ (445.36): C, 53.94; H, 5.66; N, 18.87. Found: C, 53.67; H, 5.49 N, 18.41. HPLC-MS (ESI+): 447.07 (97.2%). ^{1}H NMR (500 MHz, DMSO-d_6) δ ppm 0.86 (t, *J* = 7.4, 3H), 1.46 (qui, *J* = 7.0, 1H), 1.68 – 1.57 (m, 3H), 1.88 – 1.79 (m, 2H), 2.00 – 1.90 (m, 2H), 2.11 – 2.02 (m, 2H), 3.52 – 3.45 (m, 1H), 3.83 – 3.74 (m, 1H), 4.60 (t, *J* = 5.2, 1H), 4.66 (qui, *J* = 7.7, 1H), 6.23 (d, *J* = 8.1, 1H), 7.39 (d, *J* = 8.9, 2H), 7.88 (s,1H), 7.98 (d, *J* = 7.7, 2H), 9.52 (s, 1H). ^{13}C NMR (126 MHz, DMSO-d_6) δ ppm 11.26, 24.24, 24.44, 32.19, 32.31, 54.84, 55.47, 63.32, 113.59, 114.67, 122.35, 131.49, 137.37, 140.41, 152.24, 159.15.

N^2-(4-Amino-cyclohexyl)-9-benzyl-N^6-(4-bromo-phenyl)-*9H*-purine-2,6-diamine (6h)

Yield: 82 %. m.p.: 129-131 °C. Elemental analysis: Calcd. for $C_{24}H_{26}BrN_7$ (492.41): C, 58.54; H, 5.32; N, 19.91. Found: C, 58.66; H, 5.39 N, 19.82. HPLC-MS (ESI+): 493.5 (98.1%). ^{1}H NMR (500 MHz, DMSO-d_6) δ ppm 1.15-1.26 (m, 4H), 1.80 (d, *J*=9.0, 2H), 1.92 (d, *J*=9.0, 2H), 2.57-2.63 (m, 1H), 3.55-3.62 (m, 1H), 5.19 (s, 2H), 6.60 (s(br), 1H), 7.23-7.32 (m, 5H), 7.39 (d, *J*=8.0, 2H), 7.94 (s, 1H), 8.00 (d, *J*=8.0, 2H), 9.67 (s(br), 1H).

1-[9-Benzyl-6-(4-bromo-phenylamino)-*9H*-purin-2-ylamino]-propan-2-ol (6i)

Yield: 96 % m.p.: 148-149 °C. Elemental analysis: Calcd. for $C_{21}H_{21}BrN_6O$ (453.34): C, 55.64; H, 4.67; N, 18.54. Found: C, 55.41; H, 5.02 N, 18.20. HPLC-MS (ESI+): 454.5 (97.8%). ^{1}H NMR (300 MHz, DMSO-d_6) δ ppm 1.08 (d, *J*=6.21, 3H), 3.13-3.22 (m, 2H), 3.81 (sep, *J*=5.37, 1H), 4.67 (d, *J*=5.26, 1H), 5.24 (s, 2H), 6.61 (t, *J*=5.46, 1H), 7.24-7.44 (m, 5H), 7.42 (d, *J*=8.91, 2H), 7.98 (s, 1H), 8.01 (d, *J*=8.91, 2H), 9.64 (s(br), 1H). ^{13}C NMR (126 MHz, DMSO-d_6) δ ppm 21.92, 46.27, 49.84, 65.80, 113.74, 114.21, 122.48, 128.16, 129.15, 131.49, 137.89, 138.74, 140.33, 152.30, 159.69.

(9-Benzyl-2-morpholin-4-yl-*9H*-purin-6-yl)-(4-bromo-phenyl)-amine (6j)

Yield: 87 % m.p.: 171-172 °C. Elemental analysis: Calcd. for $C_{22}H_{21}BrN_6O$ (465.36): C, 56.78; H, 4.55; N, 18.06. Found: C, 56.53; H, 4.71 N, 17.83. HPLC-MS (ESI+): 466.5 (97.6%). ^{1}H NMR (300 MHz, DMSO-d_6) δ ppm 3.63-3.68 (m, 8H), 5.28 (s, 2H), 7.28-7.36 (m, 5H), 7.47 (d, *J*=8.82, 2H), 7.84 (d, *J*=8.82, 2H), 8.07 (s, 1H), 9.79 (s, 1H). ^{13}C NMR (76 MHz, DMSO-d_6) δ ppm 44.77, 45.77, 65.94, 113.52, 113.76, 122.22, 127.61, 127.71, 128.56, 131.01, 137.16, 139.02, 139.22, 151.33, 158.44.

[9-Benzyl-2-(4-methyl-piperazin-1-yl)-*9H*-purin-6-yl]-(4-bromo-phenyl)-amine (6k)

Yield: 88 % m.p.: 162-164 °C. Elemental analysis: Calcd. for $C_{23}H_{26}BrN_7$ (480.40): C, 57.50; H, 5.46; N, 20.41. Found: C, 57.38; H, 5.14 N, 20.11. HPLC-MS (ESI+): 481.8 (96.2%). ^{1}H NMR (300 MHz, DMSO-d_6) δ ppm 2.17 (s, 3H), 2.32-2.36 (m, 4H), 3.69-3.72 (m, 4H), 5.26 (s, 2H), 7.26-7.34 (m, 5H), 7.47 (d, *J*=8.79, 2H), 7.85 (d, *J*=8.79, 2H), 8.03 (s, 1H), 9.76 (s (br), 1H). ^{13}C NMR (76 MHz, DMSO-d_6) δ ppm 44.16, 45.78, 54.37, 113.45, 113.54, 122.11, 127.57, 127.69, 128.52, 130.98, 137.16, 138.80, 139.30, 151.31, 151.74, 158.35.

N^2-(4-Amino-cyclohexyl)-N^6-(4-bromo-phenyl)-9-(tetrahydro-pyran-2-yl)-*9H*-purine-2,6-diamine (6l)

Yield: 94 % m.p.: 114-115 °C. Elemental analysis: Calcd. for $C_{22}H_{28}BrN_7O$ (486.41): C, 54.32; H, 5.80; N, 20.16. Found: C, 54.38; H, 5.91 N, 19.84. HPLC-MS (ESI+): 488.3 (98.1%). ^{1}H NMR (500 MHz, DMSO-d_6) δ ppm 1.30 – 1.13 (m, 4H), 1.56 – 1.48 (m, 2H), 1.68 – 1.59 (m, 1H), 1.78 (d, J = 11.3, 2H), 1.97 – 1.82 (m, 3H), 2.58 – 2.49 (m, 1H), 3.63 – 3.52 (m, 1H), 3.96 (d, J = 12.4, 1H), 5.40 (d, J = 10.7, 1H), 6.60 (s, 1H), 7.40 (d, J = 8.6, 2H), 8.05 – 7.94 (m, 3H), 9.64 (s (br), 1H). ^{13}C NMR (126 MHz, DMSO-d_6) δ ppm 23.21, 25.10, 30.46, 31.75, 35.33, 50.46, 50.97, 68.18, 80.97, 80.97, 113.70, 113.82, 122.22, 131.44, 136.67, 140.40, 152.21, 158.91.

1-[6-(4-Bromo-phenylamino)-9-(tetrahydro-pyran-2-yl)-*9H*-purin-2-ylamino]-propan-2-ol (6m)

Yield: 79 %. m.p.: 127-128 °C. Elemental analysis: Calcd. for $C_{19}H_{23}BrN_6O_2$ (447.33): C, 51.01; H, 5.18; N, 18.79. Found: C, 51.12; H, 5.26 N, 18.57. HPLC-MS (ESI+): 449.2 (98.7%). ^{1}H NMR (300 MHz, DMSO-d_6) δ ppm 1.09 (d, J=6.15, 3H), 1.54-1.58 (m, 2H), 1.63-1.70 (m, 1H), 1.88-1.95 (m, 2H), 2.21-2.28 (m, 1H), 3.15-3.26 (m, 2H), 3.62-3.66 (m, 1H), 3.84 (sep, J=5.7, 1H), 3.98-4.02 (m, 1H), 4.71 (t, J=10.26, 1H), 5.47 (d, J=10.02, 1H), 6.62 (t, J=5.34, 1H), 7.43 (d, J=8.79, 2H), 8.01 (d, J=8.79, 2H), 8.06 (s, 1H), 9.64 (s(br), 1H). ^{13}C NMR (76 MHz, DMSO-d_6) δ ppm 21.30, 22.53, 24.48, 29.91, 49.24, 54.82, 65.27, 67.53, 80.33, 113.18, 113.50, 121.87, 130.87, 136.10, 139.64, 151.65, 159.02.

(4-Bromo-phenyl)-[2-morpholin-4-yl-9-(tetrahydro-pyran-2-yl)-*9H*-purin-6-yl]-amine (6n)

Yield: 72 %. m.p.: 133-134 °C. Elemental analysis: Calcd. for $C_{20}H_{23}BrN_6O_2$ (459.34): C, 52.30; H, 5.05; N, 18.30. Found: C, 51.87; H, 4.91 N, 17.94. HPLC-MS (ESI+): 461.0 (97.2%). ^{1}H NMR (300 MHz, DMSO-d_6) δ ppm 1.52-1.56 (m, 2H), 1.67-1.71 (m, 1H), 1.89-1.97 (m, 2H), 2.18-2.29 (m, 1H), 3.64-3.69 (m, 9H), 3.99 (d, J=11.43, 1H), 5.53 (d, J=10.05, 1H), 7.48 (d, J=8.76, 2H), 7.85 (d, J=8.76, 2H), 8,15 (s, 1H), 9.80 (s (br), 1H). ^{13}C NMR (76 MHz, DMSO-d_6) δ ppm 22.47, 24.51, 30.00, 44.73, 66.00, 67.53, 80.33, 113.56, 122.22, 131.01, 137.09, 139.17, 151.14, 151.32, 158.32.

(4-Bromo-phenyl)-[2-(4-methyl-piperazin-1-yl)-9-(tetrahydro-pyran-2-yl)-*9H*-purin-6-yl]-amine (6o)

Yield: 95 %. m.p.: 169-171 °C. Elemental analysis: Calcd. for $C_{21}H_{26}BrN_7O$ (472.38): C, 53.39; H, 5.55; N, 20.76. Found: C, 53.61; H, 5.28 N, 20.49. HPLC-MS (ESI+): 473.5 (99.1%). ^{1}H NMR (DMSO-d_6) δ ppm 1.53-1.56 (m, 2H), 1.63-1.72 (m, 1H), 1.88-1.92 (m, 2H), 2.18-2.22 (m, 4H), 2.33-2.38 (m, 4H), 3.65-3.72 (m, 5H), 3.98 (d, *J*=11.22, 1H), 5.56 (d, *J*=6.54, 1H), 7.48 (d, *J*=8.58, 2H), 7.84 (d, *J*=8.58, 2H), 8.13 (s, 1H), 9.76 (s(br), 1H). ^{13}C NMR (76 MHz, DMSO-d_6) δ ppm 22.46, 24.51, 30.06, 44.10, 45.79, 54.46, 67.51, 80.23, 113.44, 122.12, 131.00, 136.90, 139.24, 151.22, 158.26**.**

***N*^{2}-(4-Amino-cyclohexyl)-9-cyclopentyl-*N*^{6}-(4-pyrrolidin-1-yl-phenyl)-*9H*-purine-2,6-diamine (7a)**

Yield: 92%. m.p.: 216-217 °C. Elemental analysis: Calcd.for $C_{26}H_{36}N_8$ (460.62): C, 67.80; H, 7.88; N, 24.33. Found: C, 67.71; H, 7.49; N, 24.01. HPLC-MS (ESI+): 461.7 (99.6%). ^{1}H NMR (300 MHz, DMSO-d_6) δ ppm 1.17-1.38 (m, 2H), 1.74-2.06 (m, 14H), 2.20-2.24 (m, 4H), 2.75 (sep, *J*=4.26, 1H), 3.27-3.31 (m, 4H), 3.81 (sex, *J*=5.97, 1H), 4.69-4.79 (m, 2H), 6.56 (d, *J*=8.73, 2H), 7.36 (s(br), 1H), 7.52 (s, 1H), 7.58 (d, *J*=8.73, 2H). ^{13}C NMR (126 MHz, DMSO-d_6) δ ppm 24.38, 24.51, 25.42, 31.84, 32.31, 35.78, 48.12, 50.57, 53.14, 55.10, 111.81, 121.34, 122.41, 123.09, 129.84, 136.51, 144.22, 152.67, 158.74.

***N*^{2}-(4-Amino-cyclohexyl)-9-cyclopentyl-*N*^{6}-(4-morpholin-4-yl-phenyl)-*9H*-purine-2,6-diamine (7b)**

Yield: 88 %. m.p.: 189-191 °C. Elemental analysis: Calcd.for $C_{26}H_{36}N_8O$ (476.62): C, 65.52; H, 7.61; N, 23.51. Found: C, 65.23; H, 7.58; N, 23.11. HPLC-MS (ESI+): 476.9 (99.0%). ^{1}H NMR (500 MHz, DMSO-d_6) δ ppm 1.05 – 0.97 (m, 4H), 1.73 – 1.60 (m, 2H), 1.88 – 1.78 (m, 2H), 1.99 – 1.89 (m, 2H), 2.19 – 2.08 (m, 2H), 2.33 (dd, *J* = 13.8, J´=6.8, 2H), 3.07 (d, *J* = 3.2, 4H), 3.31 (s, 3H), 3.45 – 3.36 (m, 1H), 4.37 – 4.30 (m, 1H), 4.78 (p, *J* = 7.4, 1H), 6.89 (d, *J* = 8.4, 2H), 7.57 (d, *J* = 8.1, 2H), 8.32 (s,

1H), 10.02 (s, 1H). ^{13}C NMR (126 MHz, DMSO-d_6) δ ppm 12.52, 19.10, 24.03, 32.56, 49.08, 52.17, 52.88, 56.02, 56.55, 115.90, 119.39, 123.15, 130.87, 140.83, 148.13, 150.86, 152.78, 153.01.

N^2-(4-Amino-cyclohexyl)-9-cyclopentyl-N^6-[4-(4-ethyl-piperazin-1-yl)-phenyl]-*9H*-purine-2,6-diamine (7c)

Yield: 76 %. m.p.: 105-108°C. Elemental analysis: Calcd.for $C_{28}H_{41}N_9$ (503.70): C, 66.77; H, 8.20; N, 25.03. Found: C, 66.84; H, 8.02; N, 25.32. HPLC-MS (ESI+): 504.8 (98.4%). ^{1}H NMR (300 MHz, DMSO-d_6) δ ppm 1.16 (t, *J*=7.20, 3H,), 1.23-1.44 (m, 4H), 1.76-2.32 (m, 14H), 2.48 (q, *J*=7.20, 2H), 2.60-2.66 (m, 4H), 2.85 (m, 1H), 3.20-3.22 (m, 4H), 3.80 (m, 1H), 4.70 (d, *J*=5.25, 1H), 4.76 (qui, *J*=6.83, 1H), 6.95 (d, *J*=8.76, 1H), 7.40 (s (br), 1H), 7.45 (s, 1H), 7.66 (d, *J*=8.76, 1H).

N^2-(4-Amino-cyclohexyl)-9-cyclopentyl-N^6-(4-morpholin-4-ylmethyl-phenyl)-*9H*-purine-2,6-diamine (7d)

Yield: 94%. m.p.: 133-135 °C. Elemental analysis: Calcd.for $C_{27}H_{38}N_8O$ (490.64): C, 66.09; H, 7.81; N, 22.84. Found: C, 66.04; H, 7.59; N, 22.61. HPLC-MS (ESI+): 491.65 (98.2%). ^{1}H NMR (500 MHz, DMSO-d_6) δ ppm 1.30 – 1.05 (m, 4H), 1.69 – 1.56 (m, 2H), 2.12 – 1.72 (m, 10H), 2.27-2.32 (m, 4H), 2.53 (t, *J* = 10.4, 1H), 3.36 (s, 2H), 3.50-3.56 (m, 4H), 3.68 – 3.56 (m, 1H), 4.72 – 4.59 (sep, *J*=7.5, 1H), 6.39 (s(br), 1H), 7.15 (d, *J* = 8.0, 2H), 7.84 (s, 1H), 7.92 (d, *J* = 8.0, 2H), 9.32 (s(br), 1H). ^{13}C NMR (126 MHz, DMSO-d_6) δ ppm 24.31, 31.76, 32.29, 35.57, 50.53, 53.65, 55.34, 62.67, 66.74, 114.51, 120.25, 129.42, 131.24, 137.12, 139.90, 152.50, 158.63.

N^2-(4-Amino-cyclohexyl)-9-cyclopentyl-N^6-[4-(2-oxa-6-aza-spiro[3.3]hept-6-yl)-phenyl]-*9H*-purine-2,6-diamine (7e)

Yield: 82%. m.p.: 146-147 °C. Elemental analysis: Calcd.for $C_{27}H_{36}N_8O$ (488.63): C, 66.37; H, 7.43; N, 22.93. Found: C, 66.11; H, 7.08; N, 22.69. HPLC-MS (ESI+): 489.7 (98.3%). ^{1}H NMR (500 MHz, DMSO-d_6) δ ppm 1.67-2.07 (m, 14H), 2.11-2.18 (m, 2H), 2.45-2.50 (m, 4H), 4.71-4.74 (m, 4H), 3.92-3.94 (m, 4H), 4.83 (qui, *J*= 5.4, 1H), 5.48 (d, *J*=5.44, 1H), 6.48 (d, *J*=8.50, 2H), 7.55 (d, *J*=8.50, 2H), 8.32 (s, 1H), 9.95 (s, 1H).

N^2-(4-Amino-cyclohexyl)-N^6-[4-(4-benzyl-piperazin-1-yl)-phenyl]-9-cyclopentyl-*9H*-purine-2,6-diamine (7f)

Yield: 92%. m.p.: 149-150 °C. Elemental analysis: Calcd.for $C_{33}H_{43}N_9$ (565.77): C, 70.06; H, 7.66; N, 22.28. Found: C, 69.82; H, 7.48; N, 22.01. HPLC-MS (ESI+): 568.8 (99.9%). ^{1}H NMR (500 MHz, DMSO-d_6) δ ppm 1.28 – 1.12 (m, 8H), 1.70 – 1.58 (m, 4H), 2.11 – 1.74 (m, 19H), 2.65 – 2.57 (m, 2H), 3.02 (t, J = 9.8, 7H), 3.49 (d, J = 3.3, 9H), 3.62 – 3.54 (m, 4H), 4.69 – 4.59 (m, 2H), 6.29 (s(br), 1H), 6.82 (d, J = 8.8, 4H), 7.26 – 7.19 (m, 2H), 7.32 – 7.28 (m, 8H), 7.84 – 7.74 (m, 6H), 9.10 (s(br), 1H). ^{13}C NMR (126 MHz, DMSO-d_6) δ ppm 31.49, 32.29, 34.18, 49.62, 50.29, 53.16, 62.61, 116.25, 121.62, 127.51, 128.73, 128.73, 129.47, 133.19, 138.60, 146.85, 158.66.

N^2-(4-Amino-butyl)-9-cyclopentyl-N^6-(4-morpholin-4-ylmethyl-phenyl)-*9H*-purine-2,6-diamine (8a)

Yield: 85%. m.p.: 140-141 °C. Elemental analysis: Calcd.for $C_{25}H_{36}N_8O$ (464.61): C, 64.63; H, 7.81; N, 24.12. Found: C, 64.47; H, 7.43; N, 23.88. HPLC-MS (ESI+): 465.8 (96.7%). ^{1}H NMR (300 MHz, DMSO-d_6) δ ppm 1.38-1.66 (m, 6H), 1.87-1.92 (m, 6H), 2.07-2.09 (m, 4H), 2.53 (t, J=6.78,2H), 3.17 (q, J=6.39, 2H), 3.30 (s, 2H), 3.39-3.55 (m, 4H), 4.69 (qui, J=7.11, 1H), 6.64 (t, J=5.34, 1H), 7.18 (d, J=8.28, 2H), 7.88 (s, 1H), 7.95 (d, J=8.28, 2H), 9.34 (s (br), 1H).

N^2-(5-Amino-pentyl)-9-cyclopentyl-N^6-(4-morpholin-4-ylmethyl-phenyl)-*9H*-purine-2,6-diamine (8b)

Yield: 74%. m.p.: 118-120 °C. Elemental analysis: Calcd.for $C_{26}H_{38}N_8O$ (478.63): C, 65.24; H, 8.00; N, 23.14. Found: C, 65.56; H, 8.05; N, 22.92. HPLC-MS (ESI+): 479.90 (99.7%). ^{1}H NMR (300 MHz, DMSO-d_6) δ ppm 1.33-1.44 (m, 4H), 1.52-1.56 (m, 2H), 1.63-1.70 (m, 2H), 1.87-2.35 (m, 8H), 2.31-2.34 (m, 4H), 2.53 (t, J=6.42, 2H), 3.26 (q, J= 6.42, 2H), 3.40(s, 2H), 3.55-3.58 (m, 4H), 4.69 (qui, J=7.80, 1H), 6.60 (t, J=4.89, 1H), 7.18 (d, J=8.40, 2H), 7.88 (s, 1H), 7.95 (d, J=8.40, 2H), 9.33 (s (br), 1H). ^{13}C NMR (126 MHz, DMSO-d_6) δ ppm 24.25, 24.62, 29.79, 32.30, 33.36, 42.04, 53.64, 55.37, 62.66, 66.75, 114.56, 120.27, 129.43, 131.26, 136.98, 139.88, 152.22, 152.52, 158.20, 159.35.

N^2-(6-Amino-hexyl)-9-cyclopentyl-N^6-(4-morpholin-4-ylmethyl-phenyl)-*9H*-purine-2,6-diamine (8c)

Yield: 74%. m.p.: 135-136 °C. Elemental analysis: Calcd.for $C_{27}H_{40}N_8O$ (492.66): C, 65.82; H, 8.18; N, 22.74. Found: C, 65.96; H, 8.02; N, 22.64. HPLC-MS (ESI+): 493.93 (99.4%). ^{1}H NMR (500 MHz, DMSO-d_6) δ ppm 1.25-1.34 (m, 6H), 1.51-1.57 (m, 2H), 1.63-1.70 (m, 2H), 1.87-2.09 (m, 6H), 2.31-2.35 (m, 4H), 3.00 (s(br), 2H), 3.26 (q, *J*= 6.75, 2H), 3.39 (s, 2H), 3.53-3.59 (m, 4H), 4.69 (qui, *J*=6.96, 1H), 6.62 (t, *J*=6.18, 1H), 7.17 (d, *J*=8.25, 2H), 7.88 (s, 1H), 7.95 (d, *J*=8.25, 2H), 9.32 (s(br), 1H). ^{13}C NMR (126 MHz, DMSO-d_6) δ ppm 24.26, 26.87, 27.18, 29.94, 32.29, 33.48, 41.97, 53.64, 55.40, 62.67, 66.76, 114.57, 120.26, 129.41, 131.25, 136.98, 139.89, 152.22, 152.52, 159.36.

N^2-Benzyl-9-cyclopentyl-N^6-(4-morpholin-4-ylmethyl-phenyl)-*9H*-purine-2,6-diamine (8d)

Yield: 48 %. m.p.: 173-175 °C. Elemental analysis: Calcd.for $C_{28}H_{33}N_7O$ (483.61): C, 69.54; H, 6.88; N, 20.27. Found: C, 69.28; H, 7.07; N, 20.02. HPLC-MS (ESI+): 484.7 (96.5%). ^{1}H NMR (500 MHz, DMSO-d_6) δ ppm 1.71–1.58 (m, 2H), 1.87 – 1.77 (m, 4H), 2.02 – 1.91 (m, 2H), 2.19 – 2.06 (m, 2H), 3.09 – 2.96 (m, 2H), 3.14-3.18 (m, 2H), 3.81 – 3.71 (m, 2H), 3.90 (d, *J* =12.1, 2H), 4.10 (t, *J* = 5.6, 2H), 4.20 (s, 2H), 4.50 (s, 2H), 4.80(qui, *J*=7.0, 1H), 7.18-7.21 (m, 2H), 7.27–7.38 (m, 7H), 7.59–7.47 (m, 2H), 8.34 (s, 1H), 9.03 (s, 1H), 9.62 (s, 1H). ^{13}C NMR (126 MHz, DMSO-d_6) δ ppm 24.00, 31.82, 45.20, 50.31, 50.95, 59.06, 63.56120.14, 127.17, 127.24, 127.78, 128.75, 128.79, 129.14, 129.45, 130.67, 132.39, 132.61, 140.14, 140.60.

9-Cyclopentyl-N^2-(4-methoxy-benzyl)-N^6-(4-morpholin-4-ylmethyl-phenyl)-*9H*-purine-2,6-diamine (8e)

Yield: 64 %. m.p.: 228-230 °C. Elemental analysis: Calcd.for $C_{29}H_{34}N_6O_2$ (513.63): C, 69.85; H, 6.87; N, 16.85. Found: C, 69.54; H, 6.59; N, 16.91. HPLC-MS (ESI+): 514.61 (95.5%). ^{1}H NMR (500 MHz, DMSO-d_6) δ ppm 1.68 – 1.58 (m, 2H), 1.86 – 1.78 (m, 2H), 1.99 – 1.89 (m, 2H), 2.10 – 2.01 (m, 2H), 2.28-2.32 (s, 4H), 3.51-3.56 (m, 4H), 3.65 (s, 3H), 3.71 – 3.68 (m, 2H), 4.38 (d, *J* = 6.0 2H), 4.66 (qui, *J* = 7.5, 1H), 6.80 (d, *J* = 8.5, 2H), 6.85 - 7.12 (m, 4H), 7.24 (d, *J* = 6.5, 3H), 7.82 (s, 2H),

7.86 (s, 1H), 9.30 (s, 1H). ^{13}C NMR (126 MHz, DMSO-d_6) δ ppm 24.19, 32.23, 44.64, 53.61, 55.51, 62.62, 66.74, 113.91, 114.09, 120.37, 128.91, 129.14, 129.45, 129.91, 131.31, 133.65, 137.18, 139.67, 152.50, 158.39, 159.11.

(9-Cyclopentyl-2-morpholin-4-yl-*9H*-purin-6-yl)-(4-morpholin-4-ylmethyl-phenyl)-amine (8f)

Yield: 96%. m.p.: 274-276 °C. Elemental analysis: Calcd.for $C_{25}H_{33}N_7O_2$ (463.58): C, 64.77; H, 7.18; N, 21.15. Found: C, 64.69; H, 7.01; N, 21.42. HPLC-MS (ESI+): 465.69 (99.8%). ^{1}H NMR (500 MHz, DMSO-d_6) δ ppm 1.62-1.66 (m, 2H), 1.80-1.87 (m, 2H), 1.90-1.98 (m, 2H), 2.08-2.12 (m, 2H), 2.29-2.33 (m, 4H), , 3.36 (s, 2H), 3.52-3.55 (m, 4H), 3.62-3.65 (m, 1H), 4.71 (qui, *J*=7.5, 1H), 7.18 (d, *J*=8.00, 2H), 7.80 (d, *J*=8.00, 2H), 7.96 (s, 1H), 9.50 (s, 1H). ^{13}C NMR (126 MHz, DMSO-d_6) δ ppm 24.31, 32.36, 45.44, 53.69, 55.45, 62.66, 66.60, 66.74, 114.90, 120.42, 129.54, 131.72, 138.11, 139.41, 151.92, 152.16, 158.77

[9-Cyclopentyl-2-(4-methyl-piperazin-1-yl)-*9H*-purin-6-yl]-(4-morpholin-4-ylmethyl-phenyl)-amine (8g)

Yield: 96%. m.p.: 248-250 °C. Elemental analysis: Calcd.for $C_{25}H_{33}N_7O_2$ (476.62): C, 65.52; H, 7.61; N, 23.51. Found: C, 65.74; H, 7.92; N, 23.37. HPLC-MS (ESI+): 478.83 (99.7%). ^{1}H NMR (500 MHz, DMSO-d_6) δ ppm 1.10 (s, 3H), 1.62-1.69 (m, 2H), 1.83-1.90 (m, 2H), 1.90-1.96 (m, 2H), 2.08-2.114 (m, 2H), 2.19 (s, 3H), 2.28-2.32 (m, 4H), 2.34-2.38 (m, 4H), 3.36 (s, 2H), 3.50-3.55 (m, 4H), 3.65-3.69 (m, 4H), 4.70 (qui, *J*=7.50, 1H), 7.18 (d, *J*=8.50, 2H), 7.79 (d, *J*=8.50 2H), 7.95 (s, 1H), 9.47 (s, 1H). ^{13}C NMR (126 MHz, DMSO-d_6) δ ppm 24.29, 32.39, 44.73, 46.34, 53.68, 54.97, 55.35, 62.65, 66.73, 114.66, 120.44, 129.54, 131.64, 137.92, 139.47, 152.01, 152.13, 158.67.

(9-Cyclopentyl-2-piperidin-1-yl-*9H*-purin-6-yl)-(4-morpholin-4-ylmethyl-phenyl)-amine (8h)

Yield: 96%. m.p.: 163-164 °C. Elemental analysis: Calcd.for $C_{26}H_{35}N_7O$ (461.60): C, 67.65; H, 7.64; N, 21.24. Found: C, 67.29; H, 7.38; N, 21.03. HPLC-MS (ESI+): 463.78 (99.7%). ^{1}H NMR (500 MHz, DMSO-d_6) δ ppm 1.20 (s, 1H), 1.71 – 1.59 (m, 2H), 1.89 – 1.79 (m, 2H), 1.95 (td, *J* = 14.4, 7.0, 2H), 2.10 (td, *J* = 11.7, 6.7, 2H), 2.31 (s, 4H), 3.28 (s, 1H), 3.36 (s, 2H), 3.53 (t, *J* = 4.4, 4H), 3.68 –

3.61 (m, 9H), 4.71 (p, *J* = 7.7, 1H), 7.18 (d, *J* = 8.5, 2H), 7.80 (d, *J* = 8.5, 2H), 7.96 (s, 1H), 9.50 (s, 1H). ^{13}C NMR (126 MHz, DMSO-d_6) δ ppm 24.31, 32.36, 45.43, 53.69, 55.44, 62.65, 66.59, 66.73, 114.89, 120.49, 129.54, 131.72, 138.10, 139.40, 151.91, 152.15, 158.76.

2-[9-Cyclopentyl-6-(4-morpholin-4-ylmethyl-phenylamino)-*9H*-purin-2-ylamino]-ethanol (8i)

Yield: 94 %. m.p.: 127-128 °C. Elemental analysis: Calcd.for $C_{23}H_{31}N_7O_2$ (437.54): C, 63.14; H, 7.14; N, 22.41. Found: C, 63.28; H, 7.01; N, 22.30. HPLC-MS (ESI+): 439.60 (98.6%). ^{1}H NMR (500 MHz, DMSO-d_6) δ ppm 1.74 – 1.57 (m, 4H), 1.89 – 1.76 (m, 2H), 1.99 – 1.89 (m, 2H), 2.14 – 2.01 (m, 2H), 2.30 (s, 4H), 3.32 – 3.25 (s, 2H), 3.49 – 3.43 (m, 2H), 3.53 (s, 4H), 4.47 (t, *J* = 4.4, 1H), 4.66 (qui, *J*=7.5, 1H), 6.54 (t, *J* = 5.1, 1H), 7.15 (d, *J* = 8.2, 2H), 7.86 (s, 1H), 7.91 (d, *J* = 8.2, 2H), 9.30 (s, 1H). ^{13}C NMR (126 MHz, DMSO-d_6) δ ppm 24.21, 32.34, 33.07, 39.14, 53.64, 55.34, 59.43, 62.65, 66.73, 114.52, 120.26, 129.51, 131.27, 136.96, 139.83, 152.13, 152.50, 159.40.

3-[9-Cyclopentyl-6-(4-morpholin-4-ylmethyl-phenylamino)-*9H*-purin-2-ylamino]-propan-1-ol (8j)

Yield: 96 %. m.p.: 136-139 °C. Elemental analysis: Calcd.for $C_{24}H_{33}N_7O_2$ (451.56): C, 63.84; H, 7.37; N, 21.71. Found: C, 63.49; H, 7.54; N, 21.42. HPLC-MS (ESI+): 452.63 (97.8%). ^{1}H NMR (500 MHz, DMSO-d_6) δ ppm 1.70 – 1.59 (m, 3H), 1.88 – 1.80 (m, 3H), 1.99 – 1.89 (m, 3H), 2.14 – 2.03 (m, 3H), 2.30 (s, 6H), 4.70 – 4.61 (m, 3H), 6.42 (t, *J* = 5.2, 1H), 7.15 (d, *J* = 8.1, 3H), 7.87 (s, 1H), 7.89 (d, *J* = 8.5, 3H), 9.31 (s, 1H). ^{13}C NMR (126 MHz, DMSO-d_6) δ ppm 24.22, 32.33, 44.63, 53.65, 55.36, 60.63, 62.66, 66.73, 120.29, 129.52, 131.29, 137.07, 139.78, 152.52, 159.33.

4-[9-Cyclopentyl-6-(4-morpholin-4-ylmethyl-phenylamino)-*9H*-purin-2-ylamino]-butan-1-ol (8k)

Yield: 88 %. m.p.: 119-121 °C. Elemental analysis: Calcd.for $C_{25}H_{35}N_7O_2$ (451.56): C, 64.49; H, 7.58; N, 21.06. Found: C, 64.49; H, 7.62; N, 20.85. HPLC-MS (ESI+): 466.49 (98.4%). ^{1}H NMR (500 MHz, DMSO-d_6) δ ppm 1.45 (qui, *J* = 6.5, 2H), 1.53 (qui, *J* = 6.5, 2H), 1.69 – 1.60 (m, 2H), 1.89 – 1.77 (m, 2H), 2.00 – 1.89 (m, 2H), 2.12 – 2.02 (m, 2H), 2.28-2.32 (m, 4H), 3.24 (q, *J* = 6.5, 2H), 3.48

(s, 2H), 3.51-3.57(m, 4H), 4.38 (t, *J* = 5.0, 1H), 4.66 (qui, *J*=7.0, 1H), 6.58 (t, *J* = 5.4, 1H), 7.15 (d, *J* = 8.3, 2H), 7.85 (s, 1H), 7.91 (d, *J* = 8.3, 2H), 9.29 (s, 1H). ^{13}C NMR (126 MHz, DMSO-d_6) δ ppm 24.25, 26.52, 30.76, 32.30, 41.77, 53.63, 55.36, 61.25, 62.72, 66.73, 112.78, 114.55, 120.24, 129.49, 131.26, 137.00, 139.92, 152.48, 159.37.

N^2-(4-Amino-cyclohexyl)-9-cyclopentyl-N^6-(6-morpholin-4-yl-pyridin-3-yl)-9*H*-purine-2,6-diamine (8l)

Yield: 94%. m.p.: 283-284 °C. Elemental analysis: Calcd.for $C_{25}H_{35}N_9O$ (477.61): C, 62.87; H, 7.39; N, 26.39. Found: C, 62.61; H, 7.11; N, 26.02. HPLC-MS (ESI+): 478.57 (98.2%). ^{1}H NMR (500 MHz, DMSO-d_6) δ ppm 1.29-1.49 (m, 4H), 1.77-1.79 (m, 2H), 1.97-2.04 (m, 4H), 2.21-2.26 (m, 6H), 2.86 (sep, *J*= 5.26, 1H), 3.14-3.18 (m, 4H), 3.83 (sex, *J*=4.02, 1H), 3.88-3.91 (m, 4H), 4.73 (qui, *J*= 5.74, 1H), 4.86 (d, *J*= 4.02, 1H), 6.91 (s, 1h), 7.46-7.49 (m, 2H), 8.02 (s, 1H), 8.26 (s(br), 1H). ^{13}C NMR (126 MHz, DMSO-d_6) δ ppm 30.98, 31.92, 32.27, 46.39, 49.84, 66.53, 107.07, 129.22, 131.27, 137.14, 140.49, 152.67, 155.60, 158.56.

9-Cyclopentyl-2-morpholin-4-yl-9*H*-purin-6-yl)-(6-morpholin-4-yl-pyridin-3-yl)-amine (8m)

Yield: 87%. m.p.: 220-222 °C. Elemental analysis: Calcd.for $C_{23}H_{30}N_8O$ (450.54): C, 61.31; H, 6.71; N, 24.87. Found: C, 61.54; H, 6.48; N, 24.26. HPLC-MS (ESI+): 451.57 (97.6%). ^{1}H NMR (500 MHz, DMSO-d_6) δ ppm 1.61-1.67 (m, 2H), 1.83-1.83 (m, 2H), 1.91-1.96 (m, 2H), 2.07-2.09 (m, 2H), 3.38-3.40 (m, 4H), 3.61-3.68 (m, 12H), 4.70 (qui, *J*= 5.26, 1H), 6.80 (d, *J*=9.0, 1H), 7.91-7.97 (m, 2H), 8.52 (s, 1H), 9.41 (s, 1H). ^{13}C NMR (126 MHz, DMSO-d_6) δ ppm 24.23, 32.35, 45.34, 46.28, 55.56, 66.52, 107.19, 114.70, 128.54, 130.08, 131.77, 138.03, 140.68, 151.74, 152.29, 155.81, 158.84.

N^2-(4-Amino-butyl)-9-cyclopentyl-N^6-(4-morpholin-4-yl-phenyl)-9*H*-purine-2,6-diamine (8n)

Yield: 88%. m.p.: 237-239 °C. Elemental analysis: Calcd.for $C_{24}H_{34}N_8O$ (450.58): C, 63.97; H, 7.61; N, 24.87. Found: C, 64.11; H, 7.38; N, 24.59. HPLC-MS (ESI+): 451.8 (100.0%). ^{1}H NMR (300 MHz, DMSO-*d6*) δ ppm 1.39-1.45 (m, 2H), 1.54-1.59 (m, 2H), 1.65-1.69 (m, 2H), 1.87-2.10 (m, 6H), 2.58 (t, *J*=6.60, 2H), 2.97 (s(br), 2H), 3.02-3.05 (m, 4H), 3.27 (q, *J*=6.36, 2H), 3.72-3.75 (m, 4H),

4.68 (qui, *J*=7.26, 1H), 6.86 (d, *J*=8.94, 2H), 7.81 (d, *J*= 8.94, 2H), 7.85 (s, 1H), 9.14 (s(br), 1H). ^{13}C NMR (126 MHz, DMSO-d_6) δ ppm 24.24, 27.35, 30.89, 32.32, 41.86, 49.77, 55.34, 66.71, 114.40, 115.87, 121.70, 133.41, 136.65, 146.80, 151.99, 152.59, 157.99, 159.40.

N^2-(4-amino-butyl)-9-cyclopentyl-N^6-[4-(4-ethyl-piperazin-1-yl)-phenyl]-9*H*-purine-2,6-diamine (8o)

Yield: 92%. m.p.: 163-165 °C. Elemental analysis: Calcd.for $C_{26}H_{39}N_9$ (477.65): C, 65.38; H, 8.23; N, 26.39. Found: C, 65.29; H, 7.89; N, 26.39. HPLC-MS (ESI+): 478.91 (96.7%). ^{1}H NMR (300 MHz, DMSO-d_6) δ ppm 1.02 (t, *J*=7.11, 3H), 1.38-1.42 (m, 2H), 1.51-1.57 (m, 2H), 1.63-1.68 (m, 2H), 1.85-2.09 (m, 6H), 2.35 (q, *J*=7.11, 2H), 2.55 (t, *J*=7.26, 2H), 2.98 (s(br), 2H), 3.03-3.06 (m, 4H), 3.22-3.29 (m, 6H), 4.67 (qui, *J*=7.62, 1H), 6.52 (t, *J*=5.94, 1H), 6.85 (d, *J*=8.70, 2H), 7.80 (d, *J*=8.70, 2H), 7.85 (s, 1H), 9.11 (s(br), 1H). ^{13}C NMR (76 MHz, DMSO-d_6) δ ppm 11.94, 23.62, 26.74, 31.69, 40.05, 46.28, 48.88, 51.56, 52.36, 54.28, 112.18, 115.43, 121.10, 132.43, 136.20, 146.23, 151.97, 158.81.

Kinase assays

FLT3 WT, FLT3 ITD and FLT3 D835Y were purchased from ProQinase. The kinase reactions were assayed with peptide substrate (1 mg/mL AGLT (poly(Ala,Glu,Lys,Tyr) 6:2:5:1 hydrobromide) in the presence of 1 μM ATP, 0.05 μCi [γ-^{33}P]ATP, and the test compound in a final volume of 10 μL, all in a reaction buffer (60 mM HEPES-NaOH, pH 7.5, 3 mM $MgCl_2$, 3 mM $MnCl_2$, 3 μM Na-orthovanadate, 1.2 mM DTT, 2.5 μg / 50 μL $PEG_{20.000}$). The reactions were stopped by adding 5 μL of 3% aq. H_3PO_4. Aliquots were spotted onto P-81 phosphocellulose (Whatman), washed 3× with 0.5% aq. H_3PO_4 and finally air-dried. Kinase inhibition was quantified using a FLA-7000 digital image analyzer. The concentration of the test compounds required to reduce the kinase's activity by 50 % was determined from dose-response curves and reported as the IC_{50} value.

Kinase Selectivity Profiling

Preliminary protein kinase selectivity of compound **7d** was evaluated at a single concentration (10 nM) by screening against 309 enzymes at Carna Biosciences.

Cell Culture

Human cell lines were obtained from the American Type Culture Collection or the German Collection of Microorganisms and Cell Cultures and were cultivated according to the provider's instructions. Briefly, MV4-11, MOLM-13, THP-1, U937 were maintained in RPMI-1640 medium supplemented with 10% fetal bovine serum, penicillin (100 U/mL), and streptomycin (100 µg/mL). Kasumi-1 and HCC-827 were maintained in RPMI-1640 medium supplemented with 20% fetal bovine serum, penicillin (100 U/mL), and streptomycin (100 µg/mL). K562, MCF-7 and BJ cell lines were cultivated in DMEM medium supplemented with 10% fetal bovine serum, penicillin (100 U/mL), and streptomycin (100 µg/ml). MRC-5 cells were cultivated in EMEM medium supplemented with 10% fetal bovine serum, 1% NEAA, penicillin (100 U/mL), and streptomycin (100 µg/mL). HUVEC (Human umbilical vein endothelial cells) were isolated and cultivated as described previously.[26] Murine parental Ba/F3 cell line was maintened in RPMI-1640 medium supplemented with 10% fetal bovine serum, penicillin (100 U/mL), streptomycin (100 µg/mL) and murine IL-3 (2 ng/mL). Ba/F3 FLT3-ITD cells were cultivated in RPMI-1640 medium supplemented with 10% fetal bovine serum, penicillin (100 U/mL), and streptomycin (100 µg/mL).[27] All cell lines were cultivated at 37 °C in 5% CO_2.

Cell Viability Assays

For the cytotoxicity assays, cells were treated in triplicate with six different doses of each compound for 72 h. After treatments, Calcein AM solution was added for 1 hour, and fluorescence from live cells was measured at 485 nm/538 nm (excitation/emission) using a Fluoroskan Ascent microplate reader (Labsystems). The GI_{50} value, the drug concentration lethal to 50% of the cells, was calculated from the dose response curves that resulted from the assays.

Flow Cytometry

Asynchronous cells were seeded and, after a preincubation period, treated with tested compounds for 24 hours. After the staining with propidium iodide, DNA content was analyzed by flow cytometry using a 488 nm laser (BD FACS Verse with software BD FACSuiteTM, version 1.0.6.). Cell cycle distribution was analyzed using ModFit LT (Verity Software House).

Immunoblotting

Cell lysates were prepared, then proteins were separated on SDS-polyacrylamide gels and electroblotted onto nitrocellulose membranes. After blocking, overnight incubation with specific primary antibodies, and incubation with peroxidase-conjugated secondary antibodies, peroxidase activity was detected with SuperSignal West Pico reagents (Thermo Scientific) using a CCD camera LAS-4000 (Fujifilm). The following specific antibodies were purchased from Cell signaling: anti-FLT3 (8F2) and anti-phospho-FLT3 Y589/591 (30D4), anti-phospho-FLT3 Y591 (33G6), anti-phospho-FLT3 Y842 (10A8), anti-STAT5, anti-phospho-STAT5 Y694, anti-ERK1/2, anti-phospho-ERK1/2 T202/Y204, anti-MEK1/2 (D1A5), anti-phospho-MEK1/2 S217/221 (41G9), anti-AKT (C67E7), anti-phospho-AKT S473 (D9E). Anti-GAPDH was purchased from Sigma Aldrich, and anti-PCNA (clone PC-10) was generously gifted by Dr. B. Vojtěšek.

Caspase-3/7 assay

Cellular caspase-3/7 activity was measured according to a previously published procedure.[28] MV4-11 and K562 cells were cultivated in a 96-well plate overnight. On the next day, the cells were treated with increasing concentrations of compound **7d** for 24 h. After incubation, 3x caspase-3/7 assay buffer (150 mM HEPES pH 7.4, 450 mM NaCl, 150 mM KCl, 30 mM $MgCl_2$, 1.2 mM EGTA, 1.5% Nonidet P40, 0.3% CHAPS, 30% sucrose, 30 mM DTT, 3 mM PMSF) containing 150 μM peptide substrate Ac-DEVD-AMC (Enzo Life Sciences) was added and after 2h incubation, the caspase-3/7 activity was measured using a Fluoroskan Ascent microplate reader (Labsystems) at 346 nm/442 nm (excitation/emission).

In Vivo Efficacy

Female athymic nu/nu mice (ENVIGO) were subcutaneously implanted with MV4-11 (5×10^6 cells in log-phase) in a mixture with Matrigel (Corning) on day 0. Body weights and tumor growth were assessed 3 times per week. The latter was measured by caliperation (using vernier caliper), and tumor volumes were calculated using the formula: tumor volume [mm^3] = $width^2 \times (length/2)$ [mm; mm]. The treatment began when the tumors reached a mean volume of about 640 mm^3 (approx. 14 days after inoculation). Quizartinib and **7d** were formulated in saline or acidified saline (pH 6.8 for application) and were administered as single doses of 10 mg/kg by intraperitoneal (i.p.) injection. Control animals received saline only. The tumors were harvested at various post-treatment intervals; after harvesting, they were mechanically disintegrated and lysed in ice cold lysis buffer. Proteins from the lysates (50 μg of total protein) were separated by SDS/PAGE, transferred to a nitrocellulose membrane, and immunoblotted with specific primary antibodies at 4 °C overnight. The HRP-conjugated secondary antibodies used for detection were incubated with membrane for 1 hour at RT and immunoblots were scanned using a Li-COR system (Li-COR Biosciences).

All aspects of the animal study met the accepted criteria for the care and experimental use of laboratory animals, and protocols were reviewed by the Ethical Committee of Faculty of Medicine and Dentistry, Palacky University in Olomouc and approved by the Ministry of Education, Youth and Sports of the Czech republic.

Homology Modeling and Molecular Docking

The X-ray crystal structure of FLT3 available from PDB (1RJB) is in an inactive conformation. We have therefore built the active DFG-in conformation of FLT3 by homology modeling based on the c-KIT kinase template (PDB ID: 1PKG). The dimer of active c-KIT contains two identical chains, chain A was selected. With default setting of Prime in Schrodinger 2017 we built the homology model and subjected it to energy minimization using the OPLS3 all-atom force field.[29] The docking was carried out with Glide using the homology model structure (Schrodinger Suite; Small-Molecule Drug Discovery Suite 2016-1, Schrödinger, LLC, New York, NY, 2016). FLT3 model was checked for

steric clashes as well as for correct protonation states and hydrogen bonding patterns.[30] No explicit water molecules were present. The protein grid was created using default settings. All ligands were converted from 2D to 3D using Ligprep module (Schrodinger Suite). Docking was performed with Glide (version,75103) in standard precision (SP) mode with flexible ligand docking and verified by induced fit docking (IFD) (Schrodinger Suite 2017; Schrodinger LLC, New York, NY). The first stage of IFD protocol performed an initial softened-potential docking of the ligand to rigid receptor, with van der Waals radii scaling of 0.50 for both FLT3 kinase homology model and ligands. Sampling of the protein for each of top 20 ligand poses was performed using Prime. Residues within 5Å of any ligand were refined; this consisted of the side chain conformational search and optimization, followed by full minimization of the residues and ligand. Complexes within 30.0 kcal/mol of minimum energy structure were taken forward for redocking. The related ligand was redocked into each low energy, induced-fit structure with default Glide settings.

ASSOCIATED CONTENT

Supporting Information

The Supporting Information is available free of charge on the ACS Publications website at DOI: 10.1021/acs.jmedchem …

Mean and SD values of enzyme-inhibitory and antiproliferative activities of novel compounds, preliminary kinase selectivity profile of **7d**, control experiments with quizartinib (FLT3 and its downstream signaling pathway inhibition, cell cycle in the MV4-11 cell line), quantification of phosphorylation levels in cell lysates and tumor tissue harvested from xenografts, NMR spectra of prepared compounds.

Molecular formula strings (CSV).

AUTHOR INFORMATION

Corresponding Author

*Vladimír Kryštof, Laboratory of Growth Regulators, Palacký University and Institute of Experimental Botany AS CR, Šlechtitelů 27, 783 71 Olomouc, Czech Republic. Phone: +420585634854, Fax: +420585634870. E-mail: vladimir.krystof@upol.cz

ORCID

Vladimír Kryštof: 0000-0001-5838-2118

Tomáš Gucký: 0000-0002-0489-5804

Eva Řezníčková: 0000-0003-4773-2850

Radek Jorda: 0000-0002-4905-7126

Karel Berka: 0000-0001-9472-2589

Martin Lepšík: 0000-0003-2607-8132

Author Contributions

T.G. and E. Ř. contributed equally. T.G. and V.M. prepared compounds, E.Ř. and R.J. performed biochemical and cellular experiments, T.R.M. and Z.K. performed animal experiments, V.B., K.B., H.A., M.L. performed computational experiments, V.D and V.K. designed the study and drafted the manuscript.

ACKNOWLEDGMENTS

The authors wish to acknowledge the support of the Ministry of Education, Youth and Sports of the Czech Republic (National Program of Sustainability I, LO1204), from the Large Infrastructures for Research, Experimental Development and Innovations (IT4Innovations National Supercomputing Center, LM2015070), the Ministry of Health of the Czech Republic (15-28951A), and Palacký University in Olomouc (IGA_PrF_2017_028, IGA_PrF_2018_006). HUVECs were kindly provided by prof. J. Ulrichová (Palacký University, Olomouc, Czech Republic). Murine parental Ba/F3 cells

and Ba/F3 cells stably transfected with FLT3-ITD were kindly provided by prof. J. Duyster and prof. R. Zeiser, respectively (University of Freiburg, Germany). H.A. and M.L. thank the Czech Academy of Sciences (RVO 61388963) and the European Regional Development Fund (OP RDE CZ.02.1.01/0.0/0.0/16_019/0000729).

ABBREVIATIONS USED

AML, acute myeloid leukemia; CDK, cyclin-dependent kinase; EGFR, epidermal growth factor receptor; ERK, extracellular signal-regulated kinase; FLT3, FMS-like tyrosine kinase 3; GAPDH, glyceraldehyde-3-phosphate dehydrogenase; HUVEC, human umbilical vein endothelial cells; ITD, internal tandem duplication; JAK, Janus kinase; MAPK, mitogen-activated protein kinase; PARP-1, poly (ADP-ribose) polymerase 1; PCNA, proliferating cell nuclear antigen; PDGFR, platelet-derived growth factor receptor; STAT, signal transducer and activator of transcription; TRK, tropomyosin receptor kinase

References

1. Rahman, N. Realizing the promise of cancer predisposition genes. *Nature* **2014**, *505*, 302-308.
2. Gilliland, D.; Griffin, J. The roles of FLT3 in hematopoiesis and leukemia. *Blood* **2002**, *100*, 1532-1542.
3. Carow, C.; Kim, E.; Hawkins, A.; Webb, H.; Griffin, C.; Jabs, E; Civin, C. I.; Small, D. Localization of the human stem cell tyrosine kinase-1 gene (FLT3) to 13Q12-->Q13. *Cytogenet. Cell Genet*. **1995**, *70*, 255-257.
4. Nakao, M.; Yokota, S.; Iwai, T.; Kaneko, H.; Horiike, S.; Kashima, K.; Sonoda, Y.; Fujimoto, T.; Misawa, S. Internal tandem duplication of the flt3 gene found in acute myeloid leukemia. *Leukemia* **1996**, *10*, 1911-1918.

5. Stirewalt, D. L.; Kopecky, K. J.; Meshinchi, S.; Engel, J. H.; Pogosova-Agadjanyan, E. L.; Linsley, J.; Slovak, M. L.; Willman, C. L.; Radich, J. P. Size of FLT3 internal tandem duplication has prognostic significance in patients with acute myeloid leukemia. *Blood* **2006**, *107,* 3724-3726.
6. Pemmaraju, N.; Kantarjian, H.; Ravandi, F.; Cortes, J. FLT3 inhibitors in the treatment of acute myeloid leukemia: the start of an era? *Cancer* **2011**, *117*, 3293-3304.
7. Wander, S. A.; Levis, M. J.; Fathi, A. T. The evolving role of FLT3 inhibitors in acute myeloid leukemia: quizartinib and beyond. *Ther. Adv. Hematol*. **2014**, *5,* 65-77.
8. Pemmaraju, N.; Kantarjian, H.; Andreeff, M.; Cortes, J.; Ravandi, F. Investigational FMS-like tyrosine kinase 3 inhibitors in treatment of acute myeloid leukemia. *Expert Opin. Investig. Drugs* **2014**, *23*, 943-954.
9. Zimmerman, E. I.; Turner, D. C.; Buaboonnam, J.; Hu, S.; Orwick, S.; Roberts, M. S.; Janke, L. J.; Ramachandran, A.; Stewart, C. F.; Inaba, H.; Baker, S. D. Crenolanib is active against models of drug-resistant FLT3-ITD-positive acute myeloid leukemia. *Blood* **2013**, *122*, 3607-3615.
10. Lee, L.Y.; Hernandez, D.; Rajkhowa, T.; Smith, S.C.; Raman, J. R.; Nguyen, B.; Small, D.; Levis, M. Preclinical studies of gilteritinib, a next-generation FLT3 inhibitor. *Blood* **2017**, *129*, 257-260.
11. Poulsen, A.; William, A.; Blanchard, S.; Lee, A.; Nagaraj, H.; Wang, H.; Teo, E.; Tan, E.; Goh, K. C.; Dymock, B. Structure-based design of oxygen-linked macrocyclic kinase inhibitors: discovery of SB1518 and SB1578, potent inhibitors of Janus kinase 2 (JAK2) and Fms-like tyrosine kinase-3 (FLT3). *J. Comput. Aided Mol. Des*. **2012**, *26*, 437-450.
12. Goh, K. C.; Novotny-Diermayr, V.; Hart, S.; Ong, L. C.; Loh, Y. K.; Cheong, A.; Tan, Y. C.; Hu, C.; Jayaraman, R.; William, A. D.; Sun, E. T.; Dymock, B. W.; Ong, K. H.; Ethirajulu, K.; Burrows, F.; Wood, J. M. TG02, a novel oral multi-kinase inhibitor of CDKs, JAK2 and FLT3 with potent anti-leukemic properties. *Leukemia* **2012**, *26*, 236-243.
13. Keegan, K.; Li, C.; Li, Z.; Ma, J.; Ragains, M.; Coberly, S.; Hollenback, D.; Eksterowicz, J.; Liang, L.; Weidner, M.; Huard, J.; Wang, X.; Alba, G.; Orf, J.; Lo, M. C.; Zhao, S.; Ngo, R.; Chen, A.; Liu, L.; Carlson, T.; Quéva, C.; McGee, L. R.; Medina, J.; Kamb, A.; Wickramasinghe, D.; Dai, K. Preclinical evaluation of AMG 925, a FLT3/CDK4 dual kinase inhibitor for treating acute myeloid leukemia. *Mol. Cancer Ther*. **2014**, *13*, 880-889.

14. Li, Z.; Wang, X.; Eksterowicz, J.; Gribble, M. W. Jr.; Alba, G. Q.; Ayres, M.; Carlson, T. J.; Chen, A.; Chen, X.; Cho, R.; Connors, R. V.; DeGraffenreid, M.; Deignan, J. T.; Duquette, J.; Fan, P.; Fisher, B.; Fu, J.; Huard, J. N.; Kaizerman, J.; Keegan, K. S.; Li, C.; Li, K.; Li, Y.; Liang, L.; Liu, W.; Lively, S. E.; Lo, M. C.; Ma, J.; McMinn, D. L.; Mihalic, J. T.; Modi, K.; Ngo, R.; Pattabiraman, K.; Piper, D. E.; Queva, C.; Ragains, M. L.; Suchomel, J.; Thibault, S.; Walker, N.; Wang, X.; Wang, Z.; Wanska, M.; Wehn, P. M.; Weidner, M. F.; Zhang, A. J.; Zhao, X.; Kamb, A.; Wickramasinghe, D.; Dai, K.; McGee, L. R.; Medina, J. C. Discovery of AMG 925, a FLT3 and CDK4 dual kinase inhibitor with preferential affinity for the activated state of FLT3. *J. Med. Chem*. **2014**, *57*, 3430-3449.

15. Gucký, T.; Jorda, R.; Zatloukal, M.; Bazgier, V.; Berka, K.; Řezníčková, E.; Béres, T.; Strnad, M.; Kryštof, V. A novel series of highly potent 2,6,9-trisubstituted purine cyclin-dependent kinase inhibitors. *J. Med. Chem*. **2013**, *56*, 6234-6247.

16. Zatloukal, M.; Jorda, R.; Gucky, T.; Reznickova, E.; Voller, J.; Pospisil, T.; Malinkova, V.; Adamcova, H.; Krystof, V.; Strnad, M. Synthesis and in vitro biological evaluation of 2,6,9-trisubstituted purines targeting multiple cyclin-dependent kinases. *Eur. J. Med. Chem.* **2013**, *61*, 61-72.

17. Lu, W.; Sengupta, S.; Petersen, J. L.; Akhmedov, N. G.; Shi, X. Mitsunobu coupling of nucleobases and alcohols: an efficient, practical synthesis for novel nonsugar carbon nucleosides. *J. Org. Chem*. **2007**, *72*, 5012-5015.

18. Davies, N. G.; Browne, H.; Davis, B.; Drysdale, M. J.; Foloppe, N.; Geoffrey, S.; Gibbons, B.; Hart, T.; Hubbard, R.; Jensen, M. R.; Mansell, H.; Massey, A.; Matassova, N.; Moore, J. D.; Murray, J.; Pratt, R.; Ray, S.; Robertson, A.; Roughley, S. D.; Schoepfer, J.; Scriven, K.; Simmonite, H.; Stokes, S.; Surgenor, A.; Webb, P.; Wood, M.; Wright, L.; Brough, P. Targeting conserved water molecules: design of 4-aryl-5-cyanopyrrolo[2,3-d]pyrimidine Hsp90 inhibitors using fragment-based screening and structure-based optimization. *Bioorg. Med. Chem*. **2012**, *20*, 6770-6789.

19. Zorn, J. A.; Wang, Q.; Fujimura, E.; Barros, T.; Kuriyan, J. Crystal structure of the FLT3 kinase domain bound to the inhibitor Quizartinib (AC220). *PLoS One* **2015**, *10*, e0121177.

20. Smith, C. C.; Lasater, E. A.; Lin, K. C.; Wang, Q.; McCreery, M. Q.; Stewart, W. K.; Damon, L. E.; Perl, A. E.; Jeschke, G. R.; Sugita, M.; Carroll, M.; Kogan, S. C.; Kuriyan, J.; Shah, N. P. Crenolanib is a selective type I pan-FLT3 inhibitor. *Proc. Natl. Acad. Sci. U. S. A*. **2014**, *111*, 5319-5324.

21. Smith, C. C.; Lin, K.; Stecula, A.; Sali, A.; Shah, N. P. FLT3 D835 mutations confer differential resistance to type II FLT3 inhibitors. *Leukemia* **2015**, *29*, 2390-2392.

22. Zarrinkar, P. P.; Gunawardane, R. N.; Cramer, M. D.; Gardner, M. F.; Brigham, D.; Belli, B.; Karaman, M. W.; Pratz, K. W.; Pallares, G.; Chao, Q.; Sprankle, K. G.; Patel, H. K.; Levis, M.; Armstrong, R. C.; James, J. AC220 is a uniquely potent and selective inhibitor of FLT3 for the treatment of acute myeloid leukemia (AML). *Blood* **2009**, *114*, 2984-2992.

23. Gunawardane, R. N.; Nepomuceno, R. R.; Rooks, A. M.; Hunt, J. P.; Ricono, J. M.; Belli, B.; Armstrong, R. C. Transient exposure to quizartinib mediates sustained inhibition of FLT3 signaling while specifically inducing apoptosis in FLT3-activated leukemia cells. *Mol. Cancer Ther*. **2013**, *12*, 438-447.

24. Kampa-Schittenhelm, K. M.; Heinrich, M. C.; Akmut, F.; Döhner, H.; Döhner, K.; Schittenhelm, M. M. Quizartinib (AC220) is a potent second generation class III tyrosine kinase inhibitor that displays a distinct inhibition profile against mutant-FLT3, -PDGFRA and -KIT isoforms. *Mol. Cancer* **2013**, *12*, 19.

25. Bruner, J. K.; Li, L.; Ma, H. S.; Qin, A. C. R.; Levis, M. J.; Pratz, K. W.; Pratilas, C. A.; Small, D. Signaling adaptation to TKI treatment reactivates ERK signaling in FLT3/ITD leukemia. *Blood* **2016**, *128*, 33.

26. McGregor, P. E.; Agrawal, D. K.; Edwards, J. D. Technique for assessment of leukocyte adherence to human umbilical vein endothelial cell monolayers. *J. Pharmacol. Toxicol. Methods*. **1994**, *32*, 73-77.

27. Mathew, N. R.; Baumgartner, F.; Braun, L.; O'Sullivan, D.; Thomas, S.; Waterhouse, M.; Müller, T. A.; Hanke, K.; Taromi, S.; Apostolova, P.; Illert, A. L.; Melchinger, W.; Duquesne, S.; Schmitt-Graeff, A.; Osswald, L.; Yan, K. L.; Weber, A.; Tugues, S.; Spath, S.; Pfeifer, D.; Follo, M.; Claus, R.; Lübbert, M.; Rummelt, C.; Bertz, H.; Wäsch, R.; Haag, J.; Schmidts, A.;

Schultheiss, M.; Bettinger, D.; Thimme, R.; Ullrich, E.; Tanriver, Y.; Vuong, G. L.; Arnold, R.; Hemmati, P.; Wolf, D.; Ditschkowski, M.; Jilg, C.; Wilhelm, K.; Leiber, C.; Gerull, S.; Halter, J.; Lengerke, C.; Pabst, T.; Schroeder, T.; Kobbe, G.; Rösler, W.; Doostkam, S.; Meckel, S.; Stabla, K.; Metzelder, S. K.; Halbach, S.; Brummer, T.; Hu, Z.; Dengjel, J.; Hackanson, B.; Schmid, C.; Holtick, U.; Scheid, C.; Spyridonidis, A.; Stölzel, F.; Ordemann, R.; Müller, L. P.; Sicre-de-Fontbrune, F.; Ihorst, G.; Kuball, J.; Ehlert, J. E.; Feger, D.; Wagner, E. M.; Cahn, J. Y.; Schnell, J.; Kuchenbauer, F.; Bunjes, D.; Chakraverty, R.; Richardson, S.; Gill, S.; Kröger, N.; Ayuk, F.; Vago, L.; Ciceri, F.; Müller, A. M.; Kondo, T.; Teshima, T.; Klaeger, S.; Kuster, B.; Kim, D. D. H.; Weisdorf, D.; van der Velden, W.; Dörfel, D.; Bethge, W.; Hilgendorf, I.; Hochhaus, A.; Andrieux, G.; Börries, M.; Busch, H.; Magenau, J.; Reddy, P.; Labopin, M.; Antin, J. H.; Henden, A. S.; Hill, G. R.; Kennedy, G. A.; Bar, M.; Sarma, A.; McLornan, D.; Mufti, G.; Oran, B.; Rezvani, K.; Shah, O.; Negrin, R. S.; Nagler, A.; Prinz, M.; Burchert, A.; Neubauer, A.; Beelen, D.; Mackensen, A.; von Bubnoff, N.; Herr, W.; Becher, B.; Socié, G.; Caligiuri, M. A.; Ruggiero, E.; Bonini, C.; Häcker, G.; Duyster, J.; Finke, J.; Pearce, E.; Blazar, B. R.; Zeiser, R. Sorafenib promotes graft-versus-leukemia activity in mice and humans through IL-15 production in FLT3-ITD-mutant leukemia cells. *Nat. Med*. **2018**, *24*, 282-291.

28. Carrasco, R. A.; Stamm, N. B.; Patel, B. K. One-step cellular caspase-3/7 assay. *Biotechniques* **2003**, *34*, 1064-1067.
29. Harder, E.; Damm, W.; Maple, J.; Wu, C.; Reboul, M.; Xiang, J. Y.; Wang, L.; Lupyan, D.; Dahlgren, M. K.; Knight, J. L.; Kaus, J. W.; Cerutti, D. S.; Krilov, G.; Jorgensen, W. L.; Abel, R.; Friesner, R. A. OPLS3: A force field providing broad coverage of drug-like small molecules and proteins. *J. Chem. Theory Comput*. **2016**, *12*, 281-296.
30. Halgren, T. A.; Murphy, R. B.; Friesner, R. A.; Beard, H. S.; Frye, L. L.; Pollard, W. T.; Banks, J. L. Glide: a new approach for rapid, accurate docking and scoring. 2. Enrichment factors in database screening. *J. Med. Chem*. **2004**, *47*, 1750-1759.

Table of Contents Graphic

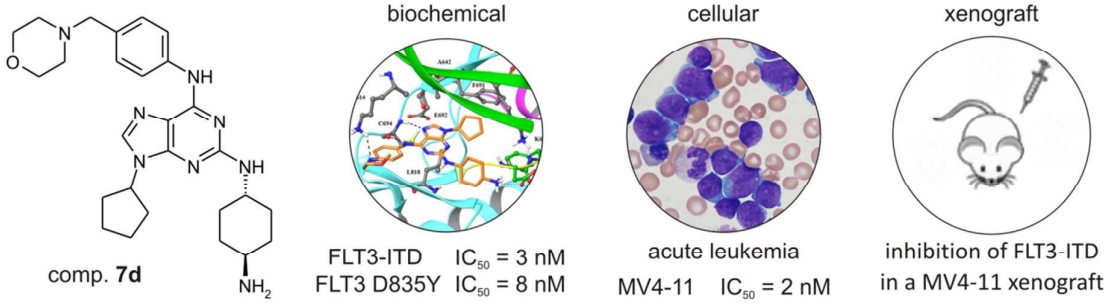

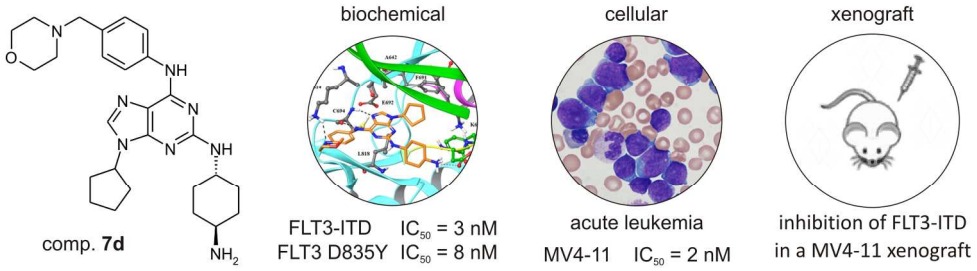

Table of contents graphic

177x52mm (300 x 300 DPI)